Application and prospect of localized electrochemical techniques for microbiologically influenced corrosion

A review

Chang, Weiwei; Qian, Hongchang; Li, Ziyu; Mol, Arjan; Zhang, Dawei

DOI
10.1016/j.corsci.2024.112246

Publication date
2024

Document Version
Final published version

Published in
Corrosion Science

Corrosion Science 236 (2024) 112246

Contents lists available at ScienceDirect

Corrosion Science

journal homepage: www.elsevier.com/locate/corsci

Application and prospect of localized electrochemical techniques for microbiologically influenced corrosion: A review

Weiwei Chang [a,b,c], Hongchang Qian [a,b,c,*], Ziyu Li [d], Arjan Mol [d], Dawei Zhang [a,b,c,*]

[a] Beijing Advanced Innovation Center for Materials Genome Engineering, Institute for Advanced Materials and Technology, University of Science and Technology Beijing, Beijing 100083, China
[b] National Materials Corrosion and Protection Data Center, University of Science and Technology Beijing, Beijing 100083, China
[c] BRI Southeast Asia Network for Corrosion and Protection (MOE), Shunde Innovation School of University of Science and Technology Beijing, Foshan 528399, China
[d] Department of Materials Science and Engineering, Delft University of Technology, Delft, Netherlands

ARTICLE INFO

Keywords:
Microbiologically influenced corrosion
Scanning electrochemical microscopy
Scanning Kelvin probe
Scanning Kelvin probe force microscopy
Scanning vibrating electrode technique
Local electrochemical impedance spectroscopy
Wire beam electrode

ABSTRACT

Microbiologically influenced corrosion (MIC) refers to the deterioration of metal surfaces as a result of the formation of microbial biofilms and metabolic activities at the biofilm/metal interface. Conventional macroscopic electrochemical techniques provide limited spatial resolution to investigate MIC which often occurs at localized environment within micro-/nanoscopic levels. Localized electrochemical techniques have received increasing attention in MIC research as a potential strategy to solve this challenge. This paper provides a focused review of localized electrochemical techniques employed in MIC studies, including their fundamentals and applications. Furthermore, their advantages and challenges as well as topics to be investigated in future are discussed.

1. Introduction

Microbiologically influenced corrosion (MIC) is one of the main problems faced by metals in atmospheric, water and soil environments, which may lead to reduced functionality, loss of structural integrity, major safety accidents and huge economic losses [1–3]. The research into MIC spans a history of more than 100 years [4]. Bacteria, eukaryotes and archaea all have the ability to cause or influence the corrosion of metals [5–7]. Most MIC studies focused on the MIC of bacteria, such as sulfate-reducing bacteria (SRB), nitrate-reducing bacteria (NRB), and iron-reducing bacteria (IRB) [8–12]. The formation of biofilm is generally considered to have important influence to MIC [13]. The adhesion of ambient macromolecular organic matter on the metal surface facilitates the initial colonization of microorganisms, and then the adsorption and proliferation of microbial cells contribute to the formation and development of biofilms [14]. Biofilms are often a combination of microbial cells, extracellular polymeric substances (EPS) and corrosion products in MIC. EPS is usually composed of proteins, polysaccharides, nucleic acids and lipids and can protect microbial cells against toxins [15,16]. The development of microbial molecular ecology and the introduction of microbial detection methods have helped us to better understand the key role of biofilms in MIC. It is worth noting that recent advancements in morphological observation and surface analysis methodologies at micro and nano scales have enabled the investigation of MIC at microscopic level, which provide pivotal information to further elucidate MIC mechanism [17].

The effects of microbial activity on MIC are mainly reflected in three aspects: 1) changing the metal surface microenvironment. The obstruction of substance diffusion to the metal surface caused by biofilms results in a non-homogeneous distribution of substances on the metal surface, such as dissolved oxygen and chloride ions, which creates conditions for the formation of concentration cell corrosion. The typical differential aeration driven corrosion mechanism is the result of such spatial difference in oxygen concentration [18]. 2) Damaging the metallic protective film. For metals with passive films, the acidic metabolites of microorganisms can dissolve the protective metal oxides [19–21]. Recent studies have also shown that microorganisms can use the passive films as extracellular electron acceptor, and this electron transfer behavior will change the chemical composition and lead to the degradation of the passive films [22]. 3) Influencing the electrochemical anodic reaction or cathodic reaction kinetics of metal corrosion. The conventional cathode depolarization mechanism describes the

* Corresponding authors at: Beijing Advanced Innovation Center for Materials Genome Engineering, Institute for Advanced Materials and Technology, University of Science and Technology Beijing, Beijing 100083, China.
E-mail addresses: qianhc@ustb.edu.cn (H. Qian), dzhang@ustb.edu.cn (D. Zhang).

https://doi.org/10.1016/j.corsci.2024.112246
Received 14 May 2024; Received in revised form 12 June 2024; Accepted 27 June 2024
Available online 27 June 2024

promoting effect of hydrogenase-containing SRB on the cathode reaction process through consuming the reduction product hydrogen [23]. Recently, the extracellular electron transfer (EET) mechanism has received extensive attention [24–27]. In a nutrient-deficient environment, electroactive microorganisms use metallic iron as an electron donor, thus accelerating the anode dissolution of steels [28]. In general, the MIC mechanisms show diversity according to different microbial species, environmental conditions and the types of metallic substrates.

MIC is a bioelectrochemical process occurring at the metal/biofilm interface. Therefore, electrochemical measurements are widely used to study MIC behavior and mechanism. Compared with scanning electron microscopy (SEM) and weight loss tests, electrochemical measurements enable continuous monitoring in MIC studies [29]. The commonly used macroelectrochemical methods include open circuit potential, linear polarization resistance, electrochemical impedance spectroscopy (EIS) and potentiodynamic polarization measurements [30–34].The time-resolved metal corrosion resistance can be obtained through fitting the electrochemical response and extracting the key parameters. In particular, the physicochemical representation of the corrosion process at the biofilm/metal interface can be inferred by combining EIS with equivalent circuit analysis [35]. However, with the development of MIC research, the limited spatial resolution of macroelectrochemical measurements hinders further progress in understanding intricate MIC mechanism. Localized corrosion is one of the main characteristics of MIC. Macroelectrochemical characterizations only provide the averaged electrochemical information of the corroding electrode surface, but ignore the electrochemical heterogeneity of the biofilm-covered electrode surface [36]. This not only prevents us from obtaining localized bioelectrochemical information in the MIC process, but also fails to effectively obtain the faint weak electrochemical signal changes at the MIC initiation stage. Thus, correct interpretation of MIC mechanisms solely on macroelectrochemical measurements remains highly challenging.

To solve this problem, localized electrochemical techniques with high sensitivity and high resolution have been implemented to study complex MIC mechanisms. They are mainly used to detect corrosion-induced electrochemical signals and biofilm metabolic behavior in MIC. In this review, we present various widely used local electrochemical techniques, including scanning electrochemical microscopy (SECM), scanning Kelvin probe (SKP) and scanning Kelvin probe force microscopy (SKPFM), scanning vibrating electrode technique (SVET), local electrochemical impedance spectroscopy (LEIS), and the wire beam electrode (WBE) technique. Fundamentals of these well-established techniques and their applications in MIC are described in this review, and the advantages and disadvantages of these techniques are discussed.

2. Fundamentals of localized electrochemical techniques

2.1. SECM

SECM was established by Bard and Engstrom's group in the 1980s, and has been applied in various fields after decades of development [37, 38]. In particular, the potential of SECM in monitoring enzyme activity and microbial metabolites has led to its consideration in the study of biological systems [39]. The schematic diagram of SECM is shown in Fig. 1**a**, which consists of a low-current bipotentiostat that provides current and potential to the probe or sample, a three-dimensional (3D) positioning system that controls the movement of the probe, an electrolytic cell that houses different electrodes and a computer [40]. Both the probe and the bottom sample can be used as working electrodes to apply current or potential for multifunctional testing. SECM can also be used in conjunction with optical microscopy systems and temperature control equipment for more accurate probe control and satisfaction of temperature requirement [41]. The high-resolution feature of SECM mainly depends on the ultramicroelectrodes (UMEs), which are often fabricated with platinum wire, carbon wire, gold wire, or silver wire that are wrapped by borosilicate glass capillary. Most of the existing studies adopted UMEs with a diameter of 5–25 μm due to its practicability and low price. UMEs have obvious advantages over macroelectrodes including a reduced ohmic potential drop and a faster steady-state response [42]. Nevertheless, the accuracy of the SECM test depends heavily on the distance between the UME tip and the sample surface as determined by the approach curves, which is not easy to obtain. Direct contact between the UME tip and the sample surface due to excessive approach will damage the probe tip and even break the insulating glass capillary. Therefore, the mechanical strength and precise control of UMEs is one of the main obstacles limiting the application of SECM.

Several major operation modes of SECM have been adopted in the study of biological systems according to different research objectives, including the feedback, redox competition, generation-collection modes. Different SECM modes are illustrated in Fig. 1**b-d**. When the UME tip is close to the insulator surface, the radial diffusion of the reactants to the tip is inhibited, resulting in a decrease in the monitoring current, which is known as negative feedback. By contrast, the reaction product O will diffuse towards the conductive surface and be converted to R, causing an increase in R flux and the rise of monitoring current, which is defined as positive feedback (Fig. 1**b**) [43]. The approach curve is obtained based on the feedback mode. Sun et al. [44,45] summarized the relationship between the distance of the probe and substrate and the detected current. Hence, feedback mode is often used to locate the vertical position of the probe with respect to the substrate surface. In MIC, feedback mode operation has the potential to obtain topographical information of biofilm surfaces, which can be adopted to study the biofilm development process. However, this morphology is relatively rough, and it is difficult to accurately represent the complex surface morphology of the biofilms by the micron-scale probe tip. The

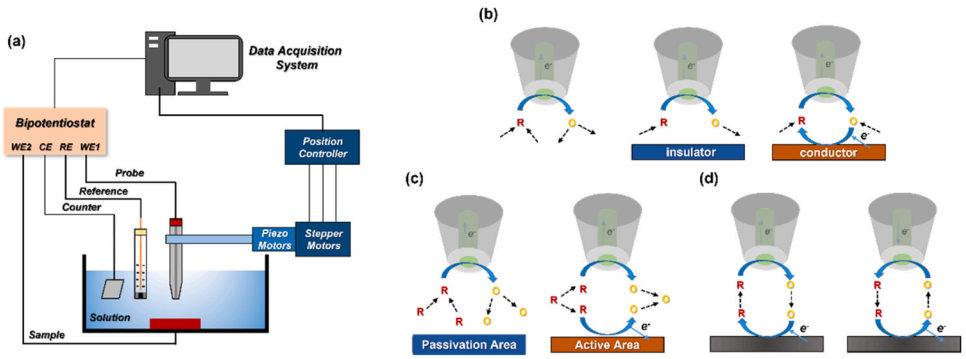

Fig. 1. (**a**) Set-up configuration of SECM; Schematic diagrams of (**b**) the feedback mode, (**c**) the redox competition mode and (**d**) the generation-collection mode.

application of nanoscale probes can greatly improve the resolution and is expected to significantly reduce and possibly solve this problem.

Redox competition mode operation is also a frequently used model in corrosion and catalytic activity studies [46,47]. By controlling the potential of the probe tip, the probe competes for the reactants with the sample surface at a relatively close distance. When the tip approaches the active area of the sample surface, such as the cathodic oxygen reduction zone of metal corrosion, the consumption of reactants by sample surface results in a decrease in the current collected by the tip (Fig. 1**c**) [48]. Controlling the distance between the tip and the substrate surface is the key to triggering "competition".

The generation-collection mode can be divided into the substrate generation/tip collection (SG/TC) mode and the tip generation/substrate collection (TG/SC) mode, as shown in Fig. 1**d**. The product of one side is captured as the reactant of the other side. In this mode, the tip can sensitively detect the diffusion layer of product O and image its spatial concentration distribution. This mode has successful applications in the study of EET process in MIC, and can be used to detect the distribution of redox electron shuttles, such as riboflavin and pyocyanin (PYO) [49,50]. In addition, the generation and collection mode can also detect the distribution of corrosion products, such as ferrous ions, which is helpful to analyze the kinetic process of anodic reactions [51].

In addition to the above common modes based on amperometric methods, several special working modes also have great potential in the study of biological systems and MIC, including alternating current (AC) mode, potentiometric mode and penetration mode [52–54]. In contrast to the constant potential methods, an alternating potential is applied to the probe tip in AC mode using a lock-in amplifier, resulting in an AC response. With positive or negative feedback under AC response, more accurate distance control can be obtained than the traditional feedback mode. The characteristics of AC mode operation unlocks important advantages in the characterization of topographical information of biofilm surfaces. In the potentiometric mode, potential signals are collected instead of current signals. Generally, an ion-selective membrane is selected according to the target test substance and applied to the UME tip. The diffusion concentration gradient of the target substance in the ion-selective membrane leads to the formation of a junction potential, which is then collected by the probe combined with the internal reference electrode. Since electrochemical reactions are not needed, the potentiometric mode does not disturb the content and distribution of the target substance, and can detect non-electroactive substances in a liquid medium, such as hydrogen and alkali [52,55]. The potentiometric mode has obvious advantages in the detection of the cathodic reduction reaction product hydrogen under anaerobic MIC, or for local pH measurements near biofilms. All of the above operating modes are aimed to provide quantitative information on electrochemical activity and presence of species above or near the biofilms, but cannot accommodate the study of substance diffusion and cell activity inside the biofilm. With the development of nanoscale UMEs, the penetration mode is expected to achieve this goal [56]. The nanoscale UME tip can penetrate the biofilm to measure ion concentration and pH distribution inside the biofilm or at the biofilm/sample interface without causing significant damage to the biofilms.

SECM stands out among various localized electrochemical techniques with its ultra-high resolution and diverse operation modes tailored for various applications. However, there are still many limitations in its application: (1) to achieve nanometer-level resolution or ion selective functionality, the intricate preparation of bespoke probes is essential, which poses a significant challenge in fabrication techniques. (2) It is difficult to differentiate between electrochemical signals and morphological alteration, which also affects accurate positioning. (3) In a complex solution system, it is difficult to maintain the long-term effectiveness of probes during in-situ testing [57,58].

2.2. SKP and SKPFM

SKP can detect the local potential distribution on the surface of metal or semiconductor through a Kelvin probe with nondestructive and non-contact features, and its principle was proposed by Kelvin in 1898 [59]. When two metals are connected with an electrical circuit and are close to each other, electrons will flow from the metal with the lower work function to the metal with higher work function, which results in a parallel plate capacitor between the two metals. The electric field of the capacitor known as contact potential difference (V_{CPD}) is equal to the difference of the metal work function ($\Delta\Phi = \Phi_1 - \Phi_2$) [60,61]. The change of the work function difference between the vibrating probe and the electrode surface can cause a change of the potential value of the capacitor. SKP counteracts this potential voltage by applying an opposite backing potential ($V_{applied}$) to the probe. The principle of V_{CPD} measurement is displayed in Fig. 2. Using this method, SKP can obtain the distribution of V_{CPD} on the local electrode surface. This potential has been reported to directly correlate with the corrosion resistance; metal surfaces with lower work function tend to be more prone to corrosion [62–65].

Although SKP enables to perform highly sensitive measurements for corrosion under thin electrolytes in air, the specific morphology of samples under the probe cannot be revealed. Nonnenmacher et al. [66] combined SKP and atomic force microscopy (AFM) to simultaneously measure the surface morphology and potential distribution of samples in 1991, which is known as SKPFM. In SKPFM, the potential difference between the probe and the electrode surface induces vibration of the probe cantilever. The system compensates for this potential difference by applying a DC voltage between the probe and the electrode, nullifying the cantilever's vibration amplitude, thus enabling the measurement of the local surface potential distribution. Relying on the AFM, two scanning processes are conducted during SKPFM measurements. During the first scan, the surface topography of the electrode surface is obtained by a semi-contact operation mode. During the second scan, the height of probe is raised by 5 nm ~ 50 nm, and the surface potential is measured in non-contact mode over the topography trajectory [67–69]. Attributed to the tiny size of the AFM probe, the SKPFM technique achieves nanoscale spatial resolution. Frankel et al. systematically studied the influence of test parameters and the surface states of the sample on the potential obtained by SKPFM, providing information of surface oxide structure and adsorption on the oxide surface with a high spatial resolution [70,71].

The signals obtained by SKPFM probes are susceptible to interference from cantilever vibrations, which exacerbates as the distance between the sample and the probe increases. Hence, SKPFM measurements are extremely surface sensitive. When the surface morphology of the sample has a relatively large variation, it can influence the accuracy of the signal [72]. Furthermore, both SKP and SKPFM are limited to measuring samples in air or under thin liquid films, which restricts their application for in situ studies on corrosion in electrolytes.

2.3. SVET

SVET is another common non-contact local corrosion detection technology. Fig. 3 shows SVET setup and probe topography. Different from SECM, SVET studies the properties and strength of corrosion reactions by measuring the current density generated by ion flow during the electrochemical corrosion reactions of metals. Originally, SVET was a technique used by biologists to measure ion flow and extracellular current in biological systems, which was introduced into corrosion research by Isaacs in the 1970s [73]. Corrosion of metals typically originates from a heterogeneous spatial distribution of the substrate microstructure and redox ions at the cathodic or anodic surface, leading to the generation of a potential gradient. SVET can be used to study redox reactions on a microscopic scale and obtain the ionic current density in the electrolyte above the corrosion region whereas the local

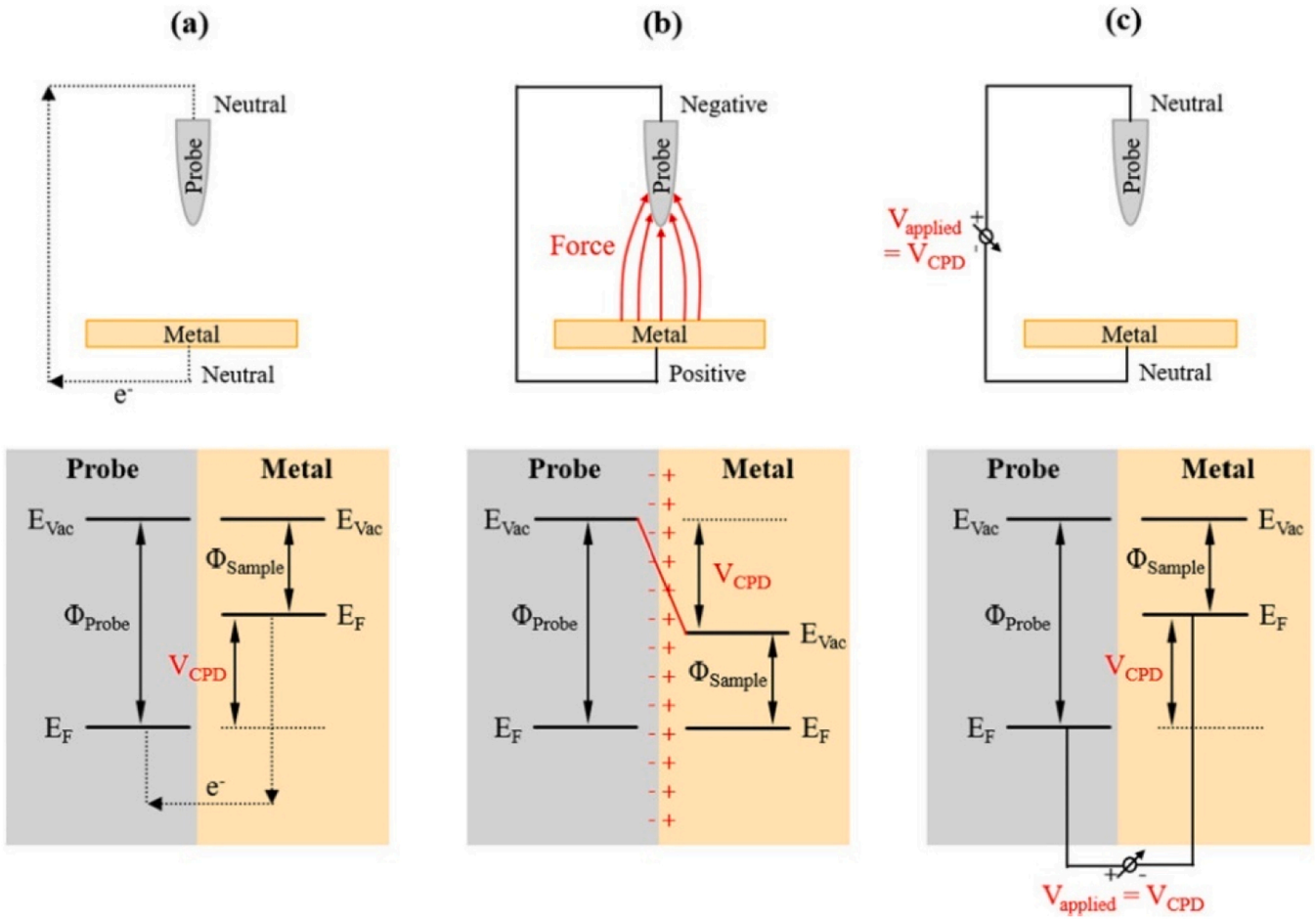

Fig. 2. The principle of V_{CPD} measurement: (**a**, **b**) the contact of two metals with different work function, (**c**) a voltage applied to counteract the contact potential difference. E_{vac} and E_F represent vacuum level and Fermi level, respectively [60].

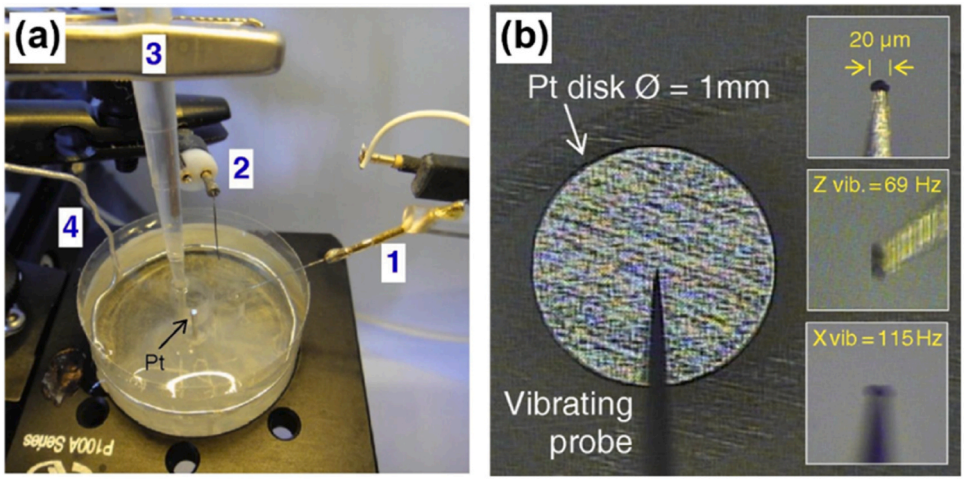

Fig. 3. (**a**) The schematic of SVET set up including 1-vibrating electrode, 2-pseudo-reference electrode, 3-Ag|AgCl reference electrode and 4-platinum wire counter electrode. (**b**) The size, shape and vibrating parameters of probe [80].

corrosion process is not affected. Therefore, SVET is widely used in corrosion research to investigate pitting corrosion, weld corrosion, galvanic corrosion, stress corrosion, corrosion inhibitor and coating failure [74–76].

Compared to SECM, current detected by SVET are not affected by the topography and it can minimize the diffusion current [77]. However, the spatial resolution for SVET is worse than that of SECM and further exploration is needed to achieve the preparation of probes with higher resolution. As yet, SVET cannot provide information about the chemical species involved in the measured currents [78,79].

2.4. LEIS

As another scanning technique using microelectrodes, LEIS was firstly introduced by Isaacs in 1992 [81]. The experimental setup of LEIS measurements is shown in Fig. 4**a**, consisting of a traditional three-electrode system (working electrode, counter electrode, and reference electrode) and dual microelectrode [82]. The traditional three-electrode system is used to apply an alternating voltage to the working electrode to excite an electric field in the electrolyte. LEIS allows measuring the local impedance of the electrode surface by measuring the AC-current density in the vicinity of the working electrode. The local current density can be calculated from the local potential gradient sensed by the dual microelectrode positioned near the active region at the electrode surface [83,84]. LEIS is capable of measuring the local impedance response of a point at different frequencies, and can also map the local impedance based on measurements at different points at a single frequency. The spatial resolution of the LEIS is governed by the dual-microelectrode, usually Pt or Ag/AgCl dual microelectrodes, and is determined by the size (the diameter) of the microelectrodes, the distance between the two sensing microelectrodes (d), and the distance between the probe and the substrate (h), as shown in Fig. 4**b** [82,85,86].

The best spatial resolution of the LEIS can reach ~10 μm, but it is still less than that of SECM. Similarly, the preparation of probes with high spatial resolution is still technically difficult due to the complex structure of the probes. LEIS testing does not rely on the presence of redox species in the solution, but it is highly susceptible to changes in the state at substrate/solution interface, such as molecular adsorption, corrosion product accumulation, etc. Additionally, the frequency domain of LEIS tests depends on the stability of the system.

2.5. WBE

The WBE is a composite electrode consisting of a specific number of metal wires arranged according to an array pattern. Different from the techniques introduced above, WBE is not exactly a typical localized electrochemical technique, but it also allows to map heterogeneous electrochemical processes on the overall electrode surface relying on numerous metal wire sensors [87–89]. The WBE is fabricated from a metallic wire bundle embedded in insulating materials, such as epoxy resin, as shown in Fig. 5 [87,90]. Each wire is an individual electrochemical sensor which allows to map the distribution of corrosion potential and corrosion current density in the nearby area [91]. In addition, the WBE technique can realize the simultaneous detection of electrochemical signals from hundreds of different metal wires, enabling it a powerful high-throughput method to provide sufficient corrosion performance data within a short time. The WBE has been widely used to investigate the local degradation of metallic materials [92,93].

The diameter of metal wires for WBE is usually in the millimeter level, which determines its lower resolution compared to various scanning probe techniques. When performing electrochemical information collection, only non-destructive electrochemical tests, such as and EIS and linear polarization resistance measurements, are usually performed to avoid mutual interference because all wires are immersed in one electrolyte.

3. Application in MIC

In this part, the application cases in the MIC field of various localized electrochemical techniques including SECM, SKP, SKPFM, SVET,LEIS and WBE are reviewed. At the end of this chapter, we concluded the technical characterization and the advantages and disadvantages of each localized technique.

3.1. SECM

EET mechanism has been extensively mentioned and developed in MIC research in the past decades. However, the research on the electron transport process at the biofilm/metal interface at the micro-nano scale still lacks effective means, which has become the bottleneck of EET mechanism research. For the research of EET processes in MIC, SECM has been applied and the data was analyzed in combination with macroscopic electrochemical characterization. Whiteley et al. [94] used SECM to detect PYO, a quorum-sensing metabolite released by *Pseudomonas aeruginosa* in a microscale 3D-printed cage. As shown in Fig. 6, an empty 3D-printed microtrap with an inner chamber (20 × 20 × 20 μm; length × width × height) was prepared. The distribution of PYO was obtained by detecting the oxidation current of reduced PYO at the microelectrode. The SECM current response suggested that a minimum number of 500 bacterial cells was required for *P. aeruginosa* to initiate quorum-sensing, and at least 2000 cells were able to stimulate quorum-sensing between adjacent *P. aeruginosa* aggregates. Although this paper mainly concerned the relationship between quorum sensing-mediated communication and the cell number, its experimental ideas provide inspiration for the configuration of MIC research design in the presence of electron shuttles which promote the EET efficiency.

Moreira et al. [95] investigated the influence of hydrogen-oxidizing bacteria *Shewanella oneidensis* on the corrosion of low carbon steel and used SECM to detect the hydrogen consumption by bacteria via the generation-collection operation mode, as shown in Fig. 7. The CV curves were obtained with a rate of 15 mV s^{-1} with a platinum probe located at 80 μm above the steel substrate in abiotic (blue curve) and biotic (red curve) conditions. The anodic peaks were found for both conditions which are ascribed to the dihydrogen oxidation. The smaller peak in biotic condition indicated that more H_2 was consumed by the *S. oneidensis*. The results suggested that *S. oneidensis* can use H_2 as an electron donor to promote localized corrosion of carbon steel.

Li et al. [49] employed SECM to detect the distribution of reduced and oxidized riboflavin over the passive steel surface covered with *S. oneidensis* MR-1 biofilms to interpret the corrosion mechanism under

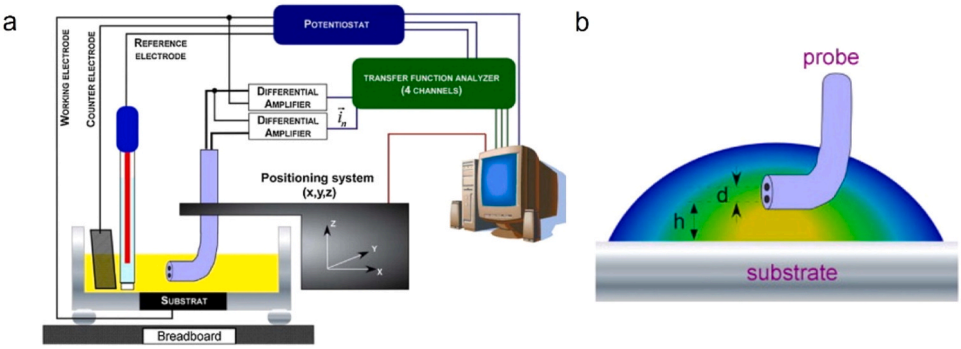

Fig. 4. (**a**) Experimental setup of LEIS measurements; (**b**) Schematic magnification of the region of the microprobe close to substrate [82].

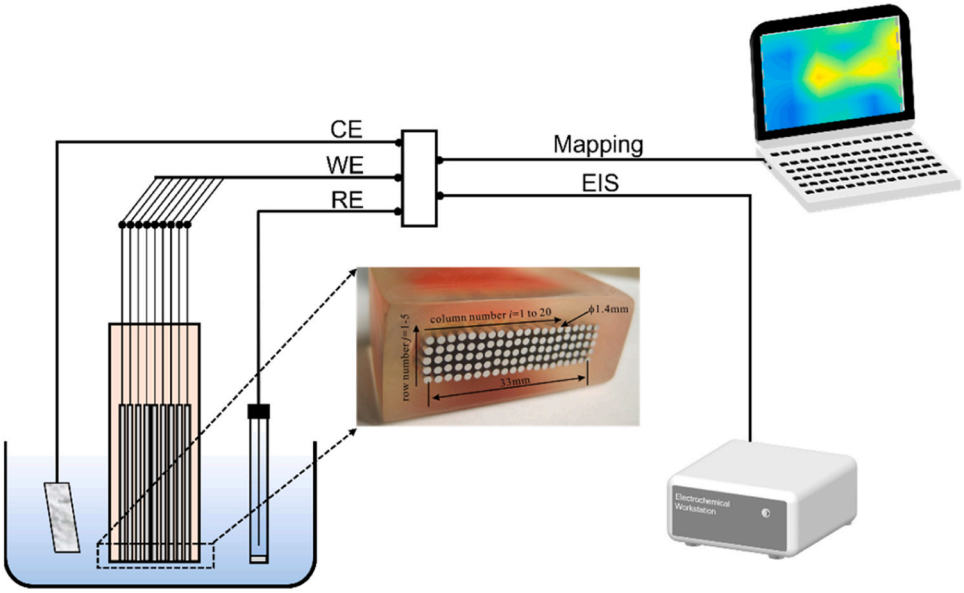

Fig. 5. Set-up configuration of WBE and the detection of electrochemical information [87,90].

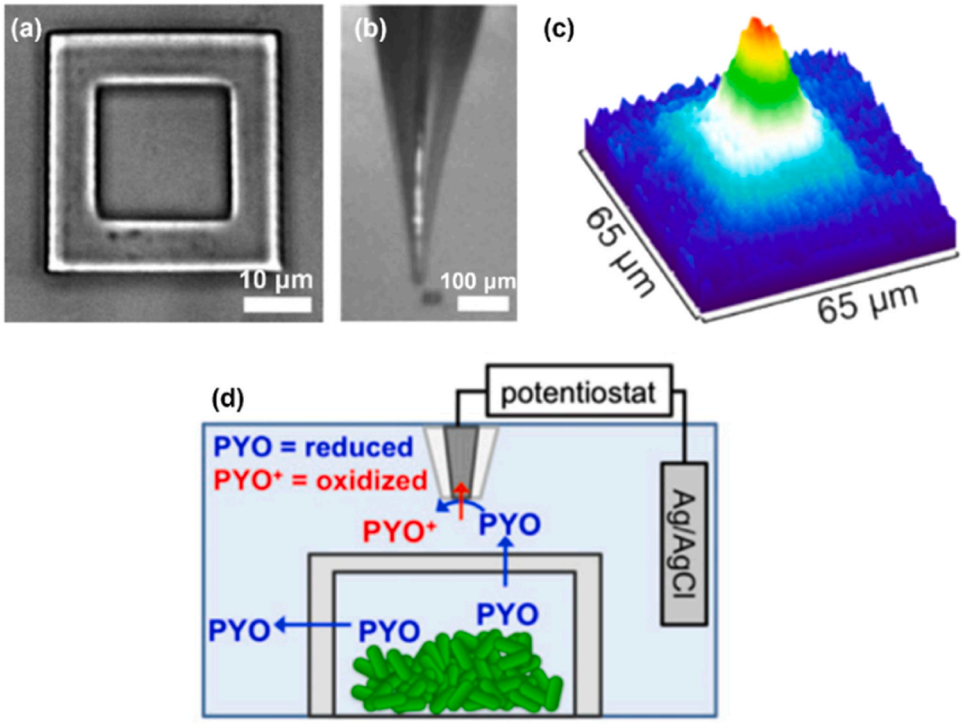

Fig. 6. (**a**) Bright-field image of an empty 3D-printed microtrap; (**b**) A video microscope image of the 5-μm-diameter SECM probe; (**c**) SECM image for PYO collected above a microtrap containing wild type (WT) *P. aeruginosa*; (**d**) Schematic of the microtrap SECM system for measuring PYO in real time [94].

riboflavin mediated MIC. To create an anaerobic atmosphere and maintain constant temperature, special monitoring devices were designed for SECM testing in this work. The SECM scanning results are presented in Fig. 8. Compared to the steel surface covered by dead cells, the distribution of riboflavin on the stainless steel surface covered by living cells showed obvious heterogeneity. In addition, riboflavin detected above the stainless steel with a natural passive film, dominantly existed in the oxidized state, while the riboflavin above an abraded stainless steel surface (passive film removed) mainly retained a reduced state. Based on the evidence of SECM, an adaptive bidirectional extracellular electron transfer mechanism between *S. oneidensis* MR-1 and stainless steel was proposed (shown in Fig. 8**b**), including inward EET (electrons transfer from materials to bacteria) and outward EET (electrons transfer from bacteria to materials). Huang et al. [50] used SECM to detect the distribution of reduced PYO and oxidized PYO on the 304 stainless steel surface when they investigated its corrosion caused by outward extracellular electron transfer of *P. aeruginosa* biofilm. When the electron acceptor (NO_3^-) was deficient, *P. aeruginosa* used PYO as the mediator to transport electrons from the inside of cells to the extracellular passive film, resulting in the reduction of ferric compounds and accelerated rupture of the passive film. This process caused the transition of the reduced PYO to the oxidized PYO on the surface of the

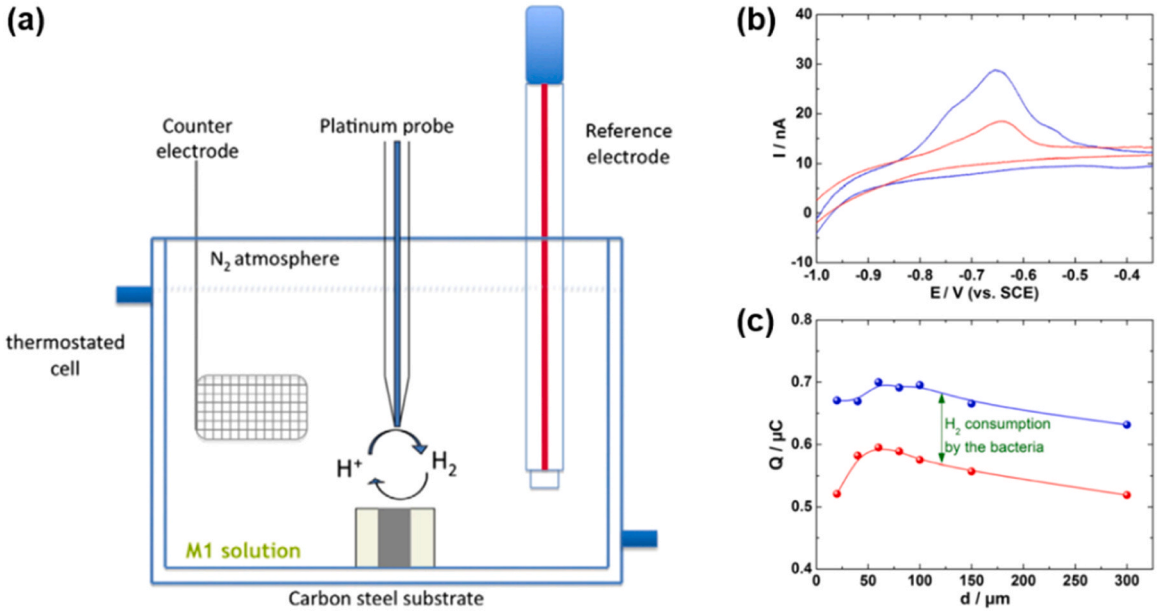

Fig. 7. (**a**) Schematic of the hydrogen consumption study of *S. oneidensis* by the generation/collection mode of SECM; (**b**) Cyclic voltammograms of the Pt microelectrode at 15 mV s^{-1} located at 80 μm above the steel substrate in abiotic (blue curve) and biotic (red curve) conditions; (**c**) Evolution of the amount of H_2 oxidized at the Pt microelectrode during the backward scan of potentials as a function of the tip-to-substrate distance [95].

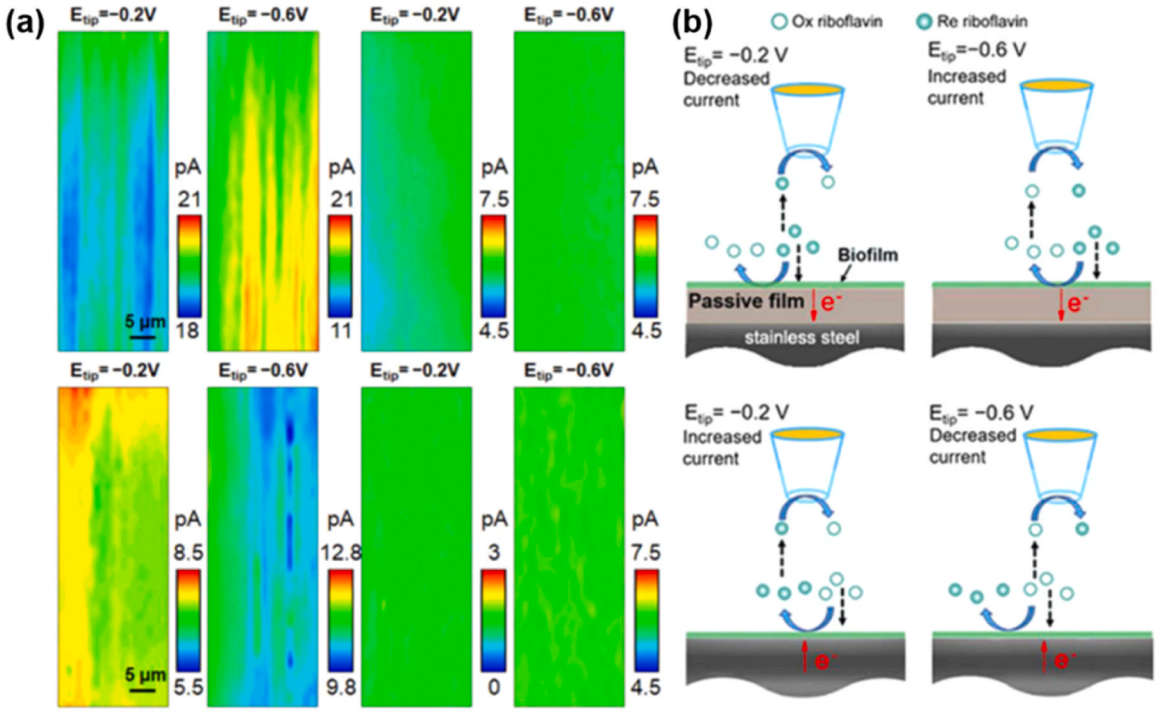

Fig. 8. (**a**) In situ SECM imaging of steel surfaces after 18 h of immersion in medium containing wild-type *S. oneidensis* MR-1; (**b**) Schematic of current variation influenced by *S. oneidensis* MR-1 on the passive and abraded stainless steel surface [49].

stainless steel. SECM results showed that the concentration of reduced PYO on the surface of stainless steel decreased in localized areas, corresponding to the increased concentration of oxidized PYO increased, which confirmed the outward EET mechanism.

In addition to the detection of microbial metabolites and metabolic processes, SECM is also adopted to characterize the corrosion protective effects of microbial minerals. Lou et al. [96] studied the MIC inhibition effect of *Shewanella putrefaciens* on Q235 carbon steel via biomineralization, by SECM analysis. *S. putrefaciens* is shown to use the cell walls as nucleation sites to induce the formation of a protective biomineralized layers on the steel surface which contained calcite and extracellular polymeric substances. An artificial scratch with a width and depth of ~40 μm was made on Q235 carbon steel surface before the immersion tests. In the SECM image, the current over the scratch region sharply reduced after 7 days and 14 days of immersion, indicating the rapid consumption of dissolved oxygen in the scratch area by the cathodic corrosion reaction on the exposed steel substrate (Fig. 9). After 7 days of immersion in the *S. putrefaciens*-inoculated medium, mineral particles

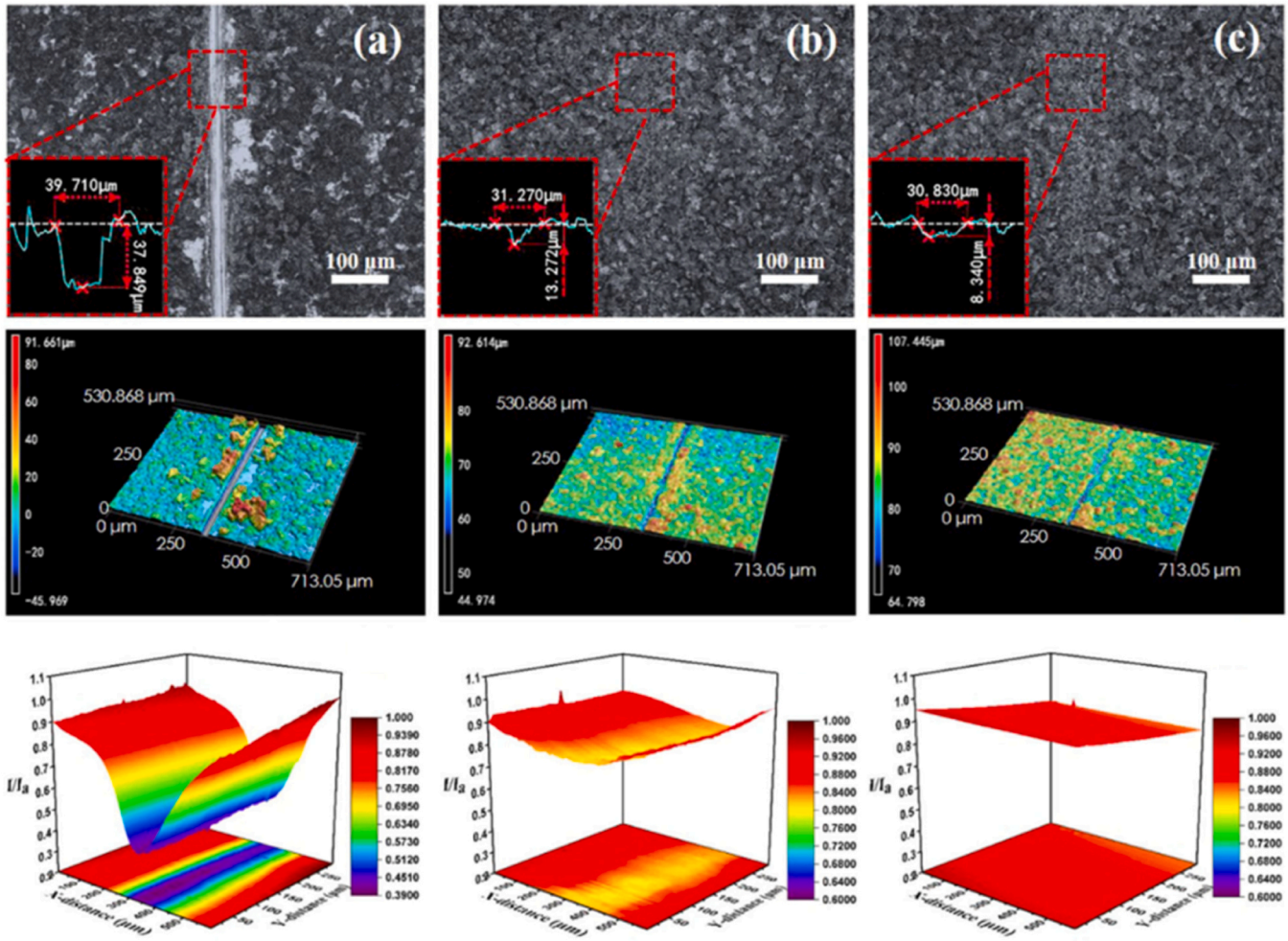

Fig. 9. Optical morphologies and SECM images of the scratch regions before and after 7 days, 14 days of immersion in the *S. putrefaciens*-inoculated media [96].

were deposited over the scratched region, effectively inhibiting the cathodic reaction and resulting in a repair efficiency of 82 % as determined by the ratio of current measured in the artificial crack region (I) to that obtained over the intact region (I_a) in SECM results. As immersion time increased to 14 days, the crack was completely repaired.

3.2. SKP and SKPFM

Since SKP and SKPFM cannot be performed in liquid environments, assessment of biofilm covered samples entail characterization of the surface potential distribution after immersion. Liu et al. [97] used SKP to investigate the potential distribution of X80 pipeline steel after 1 day and 14 days exposure in sterile and nitrate-reducing bacteria *Brevibacterium frigoritolerans*-inoculated artificial soil at 30°C. The changes in surface Kelvin potential were within 0.04 V after 1 day exposure in both sterile and inoculated soil. However, the change in surface Kelvin potential reached approximately 0.06 V in sterile soil and approximately 0.18 V in the inoculated soil after 14 days, as shown in Fig. 10**a** and **b**. The rapid increase of surface Kelvin potential under inoculated conditions suggested that the biofilms induced enhanced electronic activity of the metal surface and serious pitting corrosion occurred on the steel surface. Similarly, in their other study on MIC of X80 pipeline steel, SKP was also used to show the promoting effect of nitrate-reducing bacterium *Bacillus cereus* on localized corrosion [98]. In the SKP images, the increased Kelvin potential caused by *B. cereus* inoculation indicated that the attached biofilm can effectively hinder the electron exchange between the steel and electron acceptors in solution (Fig. 10**c** and **d**). However, the surface potential distribution was relatively dispersed after 18 days, suggesting that the *B. cereus* biofilms led to the formation of local anode and cathode regions and more severe localized corrosion.

The combination of morphology and potential characterization of SKPFM is a powerful asset in exploring the interaction of bacteria/material interface, which has important application prospects in the study of the mechanism of MIC. For example, Cui et al. [99] found that the regions at the edge of *Shewanella algae* on 201 stainless steel exhibited obvious potential drop, as shown in Fig. 11**b**. After the sessile cell was pushed away through a nano-manipulation operation, the potential drop remained (Fig. 11**e**). The line scan results indicated this potential drop to be about 13.75 mV, which was hypothesized to be the result of irreversible electron injection into the passive film on stainless steel surface from *S. algae* cells. In another research of Cui et al. [100], FIB/TEM combined with SKPFM were utilized to investigate the degradation of the passive film under a single *S. algae* cell. The results showed that the passive film under the cell almost disappeared and negative charge accumulation was observed on the 201 stainless steel substrate around the cells, which was attributed to the outward electron transfer of *S. algae*. In a recent investigation, SKPFM technique was also applied to characterize the effect of microbially-induced mineralization on the corrosion. Lou et al. [101] utilized SKPFM to compare the surface potential difference of Q235 carbon steel immersed in wild type *S. putrefaciens* inoculated medium and mutant strains (Δ*flrA* and Δ*flhG*) inoculated media. Deletion of FlrA and FlhG genes could induce the up/down-regulation of EPS expression, respectively. The steel surface with dense sediments generated under the condition of excessive EPS

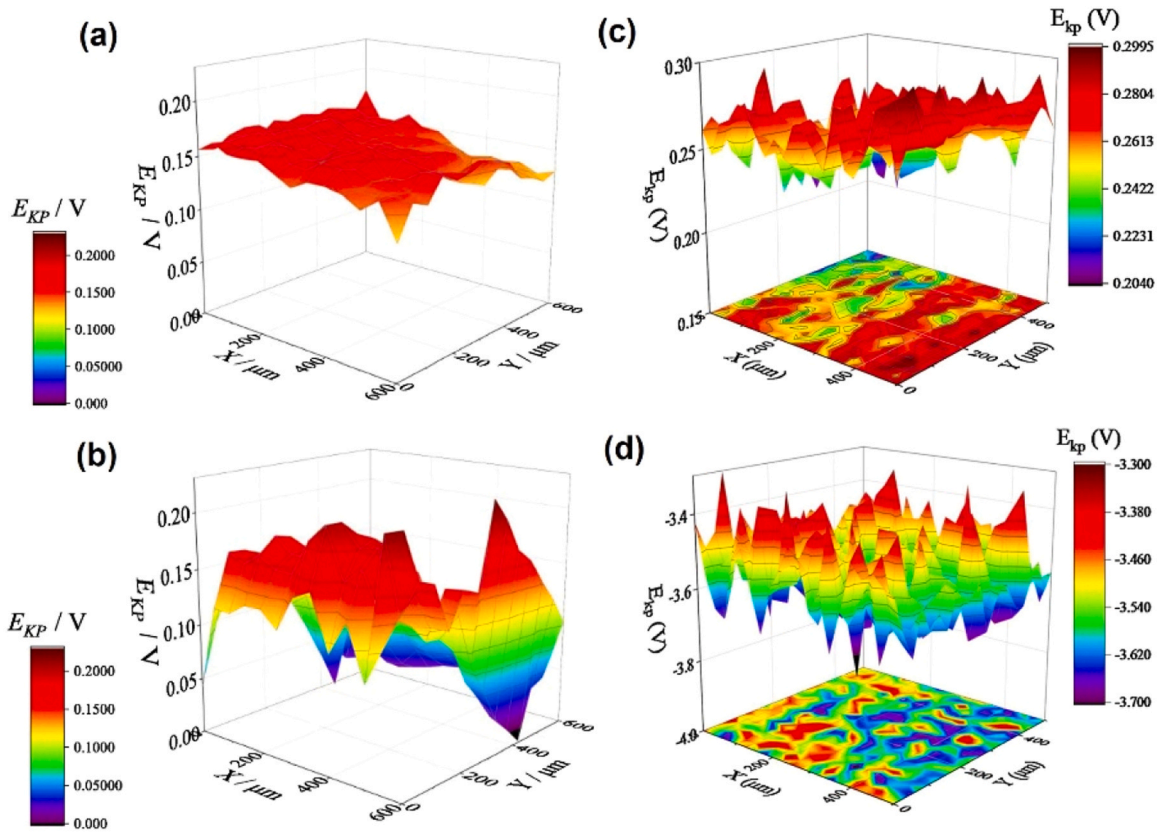

Fig. 10. SKP distribution of X80 pipeline steel in (**a**) sterile and (**b**) *B. frigoritolerans* inoculated artificial Beijing soil at 30 ℃ for 14 days. SKP distribution of X80 pipeline steel in artificial Beijing soil (**c**) with and (**d**) without *B. cereus* for 18 days [97,98].

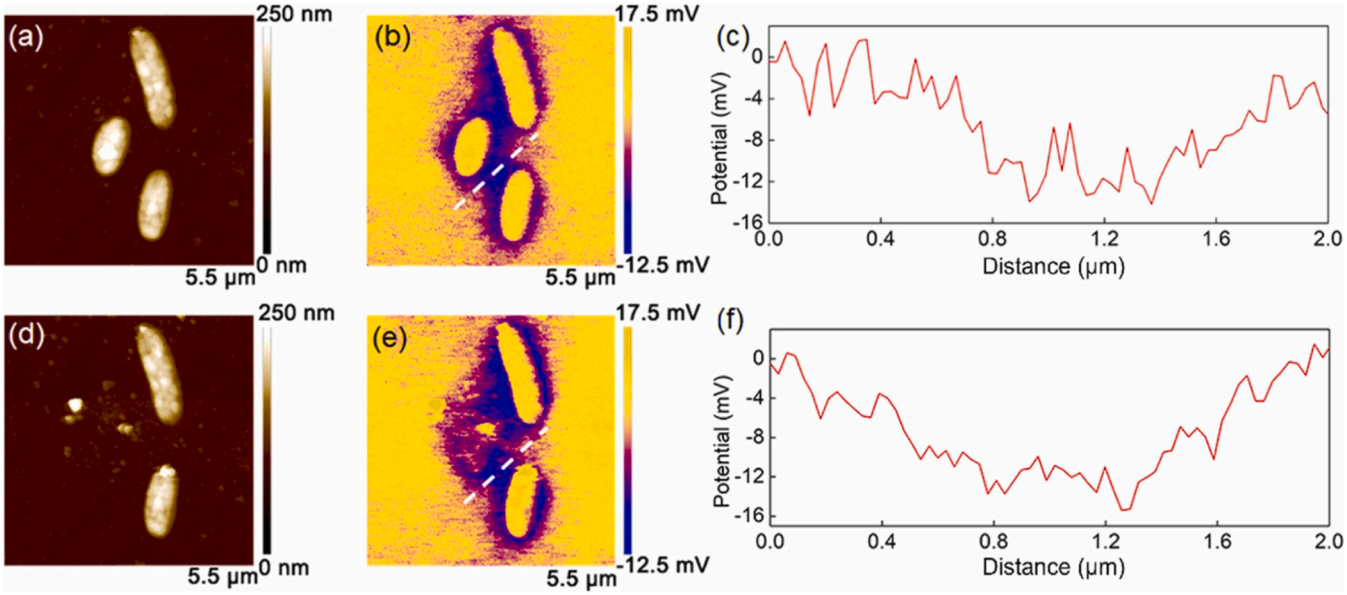

Fig. 11. Surface topography and corresponding potential distribution on 201 stainless steel immersed in *S. algae* inoculated medium for 3 days (**a**, **b**) before and (**d**, **e**) after removing the bacterial cell. (**c**, **f**) Corresponding line scan potential values [99].

exhibited the lowest potential difference, indicating the most effective corrosion inhibition.

3.3. SVET

SVET has been used to study the current variation present at metal/biofilm interfaces in MIC. Franklin et al. [102] used SVET to detect the localized corrosion of carbon steel in the presence and absence of bacteria early in 1991. In the sterile medium, high anodic current was observed and the substrate subsequently became inactive, which represented pit initiation and repassivation processes, respectively. In the inoculated medium, the localized anodic active region sustained and

spread instead of showing repassivation. This indicated that bacteria prevented the initiated anodic sites from repassivation. Liu et al. [103] adopted SVET to investigate the effect of fluid flow on the biofilm formation and MIC of pipelines caused by SRB, as shown in Fig. 12. SVET maps after 14 days of immersion showed that the potential distribution on the electrode surface was not uniform and potential peaks of up to 100 μV were observed at low flow velocity (0.2 m/s). It indicated that biofilms were formed on the electrode surface, which resulted in a heterogeneous activity of the electrode surface and a higher corrosion rate. By comparison, SVET maps at high flow velocity (1.0 m/s) exhibited a relatively uniform potential distribution with a maximum of 20 μV. It suggested that the biofilm is difficult to form under those conditions and the anodic dissolution rate was found to be low. It indicates that a low flow rate is conducive to the development of MIC.

Guo et al. [104] investigated the effect of *Bacillus subtilis* and *Pseudoalteromonas lipolytica* on the corrosion of low-alloy engineering steel. The distribution of current on the steel surface as observed by SVET analysis is relatively uniform during the tests in sterile seawater and seawater inoculated with *B. subtilis*. However, the current density observed is low and shows a maximum value of only 50 μA cm^{-2}. This uniform corrosion results from the coating of a dense layer of corrosion products. In contrast, the current distribution did not become uniform in the medium containing *P. lipolytica*, and localized current density reached 150 μA cm^{-2}, indicating that the presence of *P. lipolytica* can increase localized corrosion. In addition, Ziadi et al. [105] studied the corrosion behavior of 304 L stainless steel in treated urban wastewater using SVET. Due to heterogeneous attachment of iron-oxidizing bacteria (IOB), the current densities at anodic and cathodic regions were unevenly distributed in the SVET map after 1 h immersion. Stronger anodic regions appeared in localized area of SVET image, which represented the initiation of localized corrosion. With prolonged immersion time, the respiration of IOB locally attached to the steel surface consumed dissolved oxygen, and the corrosion product layer shields oxygen to form diffusion to the steel substrate, which lead to the generation of a differential aeration cell increasing the cathodic current density. After 11 days, the participation of SRB further intensified both anodic and cathodic corrosion processes, causing the cathodic current density to reach a maximum value of −6 μA cm^{-2} during SVET mapping.

3.4. LEIS

Moreira et al. [95] adopted LEIS to investigate the effect of iron reducing bacteria on the local corrosion of low carbon steel using H_2 as electron donor. The results of LEIS at different locations were similar, indicating that a thick and relative uniform layer of corrosion products was formed on the steel surface, and the reactivity of the interface was not dependent on the position. Shen et al. [106] investigated the effect of *B. subtilis* on the corrosion behavior of 2A14 aluminum alloy in seawater, and measured the distribution of local impedance of the 2A14 aluminum alloy surface by LEIS before and after immersion for different times in inoculated and sterile solutions. As shown in Fig. 13, the average local impedance increased dramatically after a long immersion time in the inoculated seawater, reaching 79.3 kΩ·cm^2 after 14 days. This value was much higher than that in the sterile seawater, indicating a low corrosion rate under inoculated seawater condition. The results of LEIS demonstrated the protective effect of biomineralization films produced by *B. subtilis* against corrosion in seawater environments.

Compared with macroscopic EIS, LEIS can obtain the impedance information at local regions of interest on the metal surface, which enables the analysis of local impedance changes within the biofilm attached region. Similar to macroscopic EIS, LEIS imposes only minor sinusoidal potentials to the substrate which has no significant interfering effect on the metal surface, allowing local impedance analysis without damaging the biofilm. However, due to the technical limitations of low resolution and difficult in localization, LEIS as well as SVET have not been utilized much in MIC research. These technologies still need to be further improved in the development of MIC mechanism study.

3.5. WBE

The WBE can continuously monitor the electrochemical information of different regions of the sample surface, thus it was used in many studies of MIC with heterogeneous characteristics. Dong et al. [107] used WBE to study the heterogeneous corrosion of mild steel under an

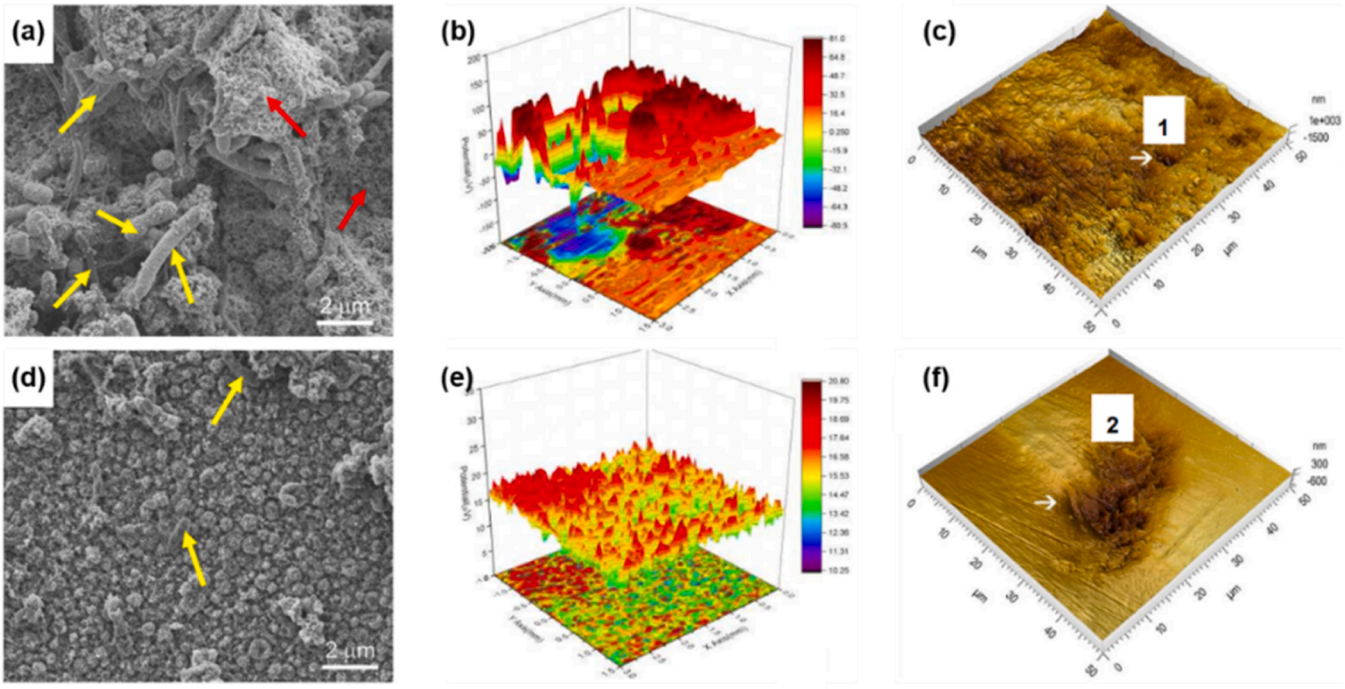

Fig. 12. (**a**) SEM morphologies, (**b**) SVET maps and (**c**) pit morphology of the steel electrode after 14 days of testing in the flowing medium at 0.2 m/s; (**d**) SEM morphologies, (**e**) SVET maps and (**f**) pit morphology of the steel electrode after 14 days in the flowing medium at 1.0 m/s [103].

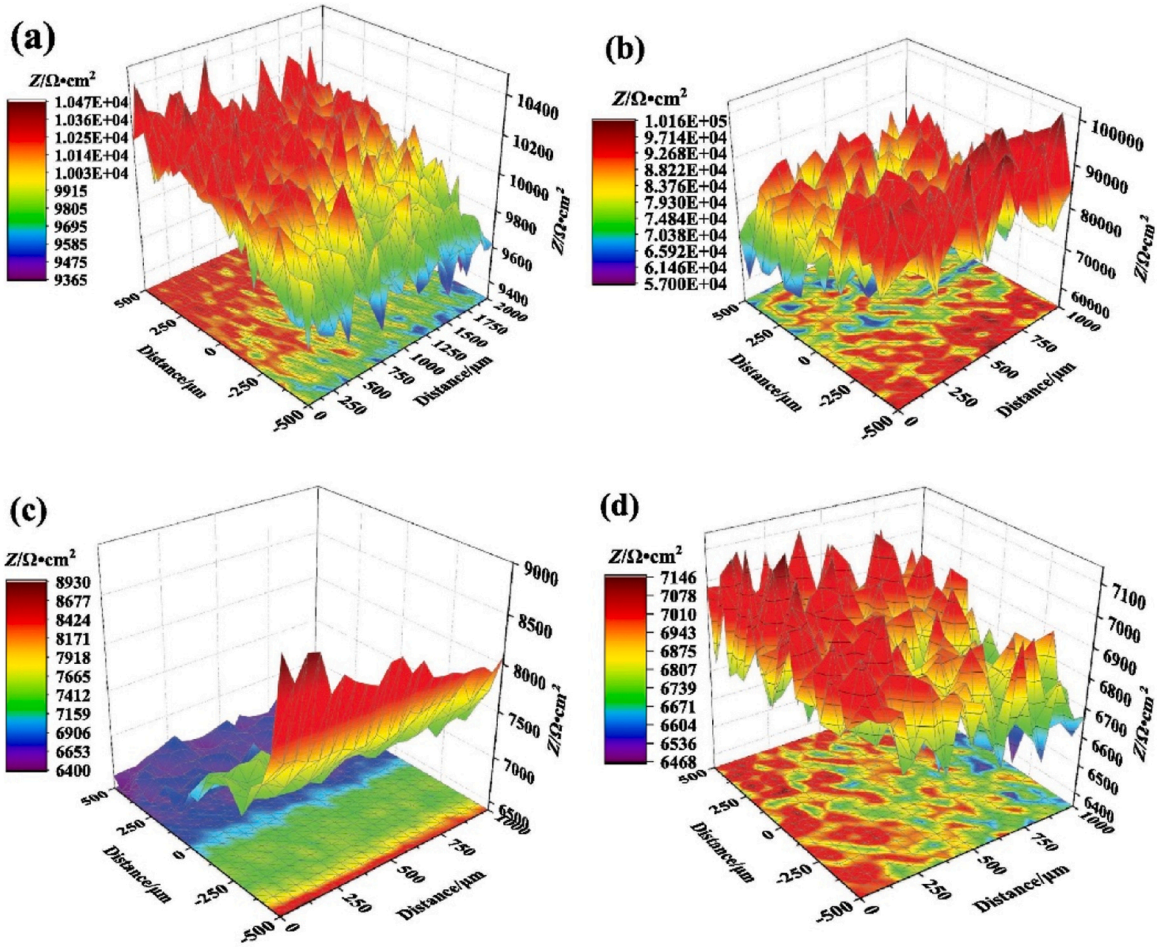

Fig. 13. LEIS of 2A14 aluminum alloy in the *B. subtilis*-inoculated medium after (**a**) 7 days and (**b**) 14 days of immersion and immersed in the sterile medium for (**c**) 7 days and (**d**) 14 days [106].

SRB biofilm. After 15 days of experiments, the potential map was very uniform and smooth, and failed to probe the localized corrosion due to the highly conductive sulfide precipitates embedded in the SRB-biofilm. However, the change of current increased to 14 μA, indicating a significant corrosion zone in the center of WBE, as shown in Fig. 14**d**. Chen et al. [108] investigated the effects of SRB on the corrosion behavior of copper in seawater using WBE. The results indicated that the presence of SRB resulted in a nonhomogeneous distribution of current across the WBE area. Wu et al. [109] studied the effect of crevice width on MIC of 316 L stainless steel with WBE, in which WBE and a convex lens formed the crack structure. The results showed that the anodic corrosion current (about 5.6×10^{-8} A) of the WBE surface in the presence of SRB was significantly higher than that in the sterile environment (about 7.5×10^{-9} A). Furthermore, crevice corrosion was more serious with the crevice width between 90–150 μm while the anodic current in the area with crevice width more than 150 μm still reached 4.5×10^{-8} A in the presence of SRB. These results indicated that SRB may increase the sensitive width range of crevice corrosion.

Moreover, the WBE current was related to the bacterial metabolic activity in SRB medium [110]. High metabolic activity of SRB results in a large variation of current and localized corrosion. Low SRB metabolic activity has little effect on the WBE current distribution and may induce uniform corrosion. Wei et al. [111] adopted WBE to study the corrosion behavior of pipelines under $CaCO_3$ deposits influenced by SRB. The results of WBE tests showed that a dense SRB biofilm slowed down the corrosion of carbon steel on the 7th day and galvanic corrosion reactions under deposition were promoted with immersion time. Liu et al. [112] investigated the corrosion behavior of deposit-covered X80 pipeline steel in seawater containing *Pseudomonas stutzeri* using WBE. The WBE galvanic current distribution between the bare sample and deposit-covered sample in the presence of *P. stutzeri* showed that the anodic current densities are smaller than those of the sterile control, which demonstrated that *P. stutzeri* can effectively inhibit steel corrosion and decrease the galvanic effects between deposit-covered and uncovered sample areas. Tuck et al. [113] utilized WBE to monitor galvanic current and corrosion potential changes in real time, enabling the evaluation of absorption of amino acids on carbon steel. The results showed greater potential value homogeneity at surface areas conditioned with amino acids, reflecting a lower surface reactivity. Combined with the detection of DNA absorption, Tuck et al. [113] proposed that a conditioning film first formed on carbon steel by DNA and amino acids and promoted the attachment of *Shewanella chilikensis*.

Apart from bacteria, the MIC induced by fungi can also be studied using WBE. Lu et al. [114] report a WBE method to study the degradation effect of fungi *Talaromyces funiculosus* on the degradation of polyurethane (PU) coating, which is shown in Fig. 15. After 14 days of immersion, the localized current density on the WBE surface can reach $\sim 10^{-3}$ A/cm^2 in the fungal inoculated medium, while the value maintained at $\sim 10^{-7}$ A/cm^2 under sterile conditions. The WBE results indicated that the degradation of the PU was more severe after being attacked by *T. funiculosus*. In addition to the localized current density, the distribution and ratio of anode and cathode regions on the sample surface over time can also be represented by WBE analysis.

According to the principle and application of each technology, Table 1 presents the comparison of different localized electrochemical techniques discussed in this review. The possible advantages and

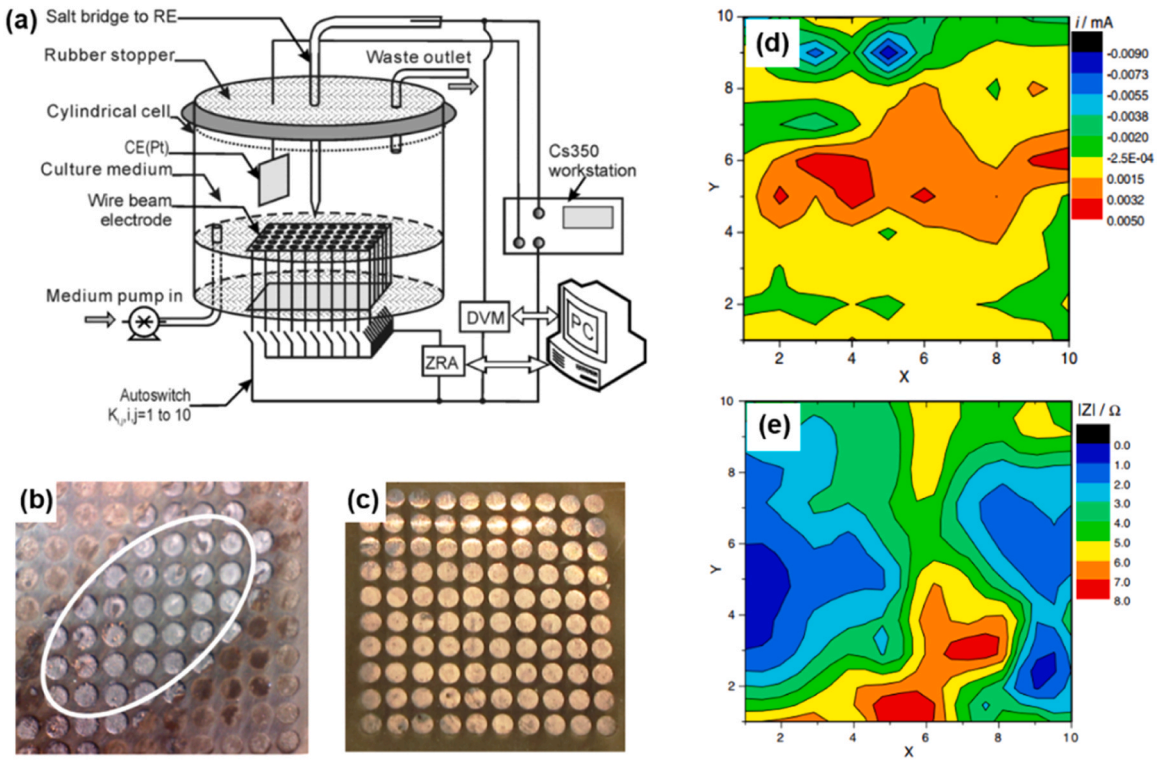

Fig. 14. (**a**) Schematic design of SRB batch reactor and corresponding electrochemical mapping device; Photographs of corroded WBE after exposed to the (**b**) SRB-incubated and (**c**) sterile medium for 15 days; (**d**) Current maps of the WBE and (**e**) modulus of impedance distribution of mild steel at frequency of 100 Hz after exposed to SRB-incubated medium for 15 days [107].

disadvantages in MIC studies are also analyzed and outlined in the table.

As mentioned above, each of the localized electrochemical techniques has its own advantages and disadvantages and meets different application requirements. In addition, some common technical difficulties need to be overcome when these technologies are applied in the research area of MIC: (1) a very tricky challenge is that the probe is difficult to locate above the biofilm attached region, except for SKPFM. It is usually necessary to configure an optical microscope to assist the probe positioning. (2) Biofilms adhering to the probe can interfere with the accuracy of the measurements. Hence, the distance between the probe and the substrate needs to be precisely controlled in the vertical direction, which increases the difficulty of the applications of SVET and LEIS. (3) Real-time electrochemical monitoring requires the exclusion of other bacterial interference. Additionally, the maintenance of temperature and humidity of the electrochemical cell is necessary to keep the activity of the living microbes. For some anaerobic bacteria, it is also hard to control the oxygen concentration in the system during the detection.

4. Conclusions and future perspectives

Materials deployed in various scenarios such as oil & gas production, marine operation and even aerospace applications are confirmed to be affected by microbiologically influenced corrosion (MIC). Even stainless steels exhibit high sensitivity to MIC apart from chloride ions, a fact that has been extensively documented through research. In reality, microbial abundance is high and the mechanisms involved are complex. Further research is still needed to better understand MIC in practical environments. Currently, most laboratory investigations focus on single bacterial strains. These studies indicate that different bacteria involved in corrosion process of materials share some common mechanisms, which can provide guidance for the prevention and control of MIC. However, the existing MIC mechanisms are still mostly inferred relying on macroscopic morphological observation and electrochemical tests. The evolution of electrochemical behavior of localized corrosion caused by MIC and the change of substance distribution at the microorganism/material interface remain insufficiently understood.

In this review, we have summarized the state of the art of localized electrochemical techniques as powerful tools to study MIC at micro- or even nanoscopic levels, including SECM, SKP, SVET, LEIS, and WBE. These techniques achieve the acquisition of signals revealing potentials, current and concentration of metabolites on electrode surface in MIC and exhibit high sensitivity and spatial resolution. The fabrication of sophisticated and miniaturized probes and the precise control of the probe movement are keys to the rapid development of localized electrochemical techniques and its application in MIC. As the size of the probe becomes nanoscale, it will be easier to spatially resolve the distribution of bioelectrochemical signals at single-cell levels and the interaction between microbial cell and materials. In addition, electrochemical characterization at single cell level can avoid the shielding effect of the biofilm on ions diffusion, which is more conductive to reveal the accurate subtle change of substances at microorganism/material interface during MIC and help to understand the process and causes of MIC.

Nevertheless, the realization of the full potential of localized electrochemical techniques in MIC research demands a deeper understanding of several important aspects: (1) precise localization, (2) long-term monitoring, and (3) testing under biofilms. First, it is difficult for most localized electrochemical techniques to accurately locate and position the probes over the electrode surface and obtain the exact topography information of the electrode surface. This leads researchers to execute intense efforts finding the appropriate test region and assessing the source and accuracy of the detected signals. This is also an operational threshold for the further application of localized electrochemical techniques in MIC research. Although SKPFM can accurately locate bacteria and then image potential distribution, it can only be performed on materials under dead bacteria in the air at present, because of the inevitable interference in the solution of electrolytes, ion

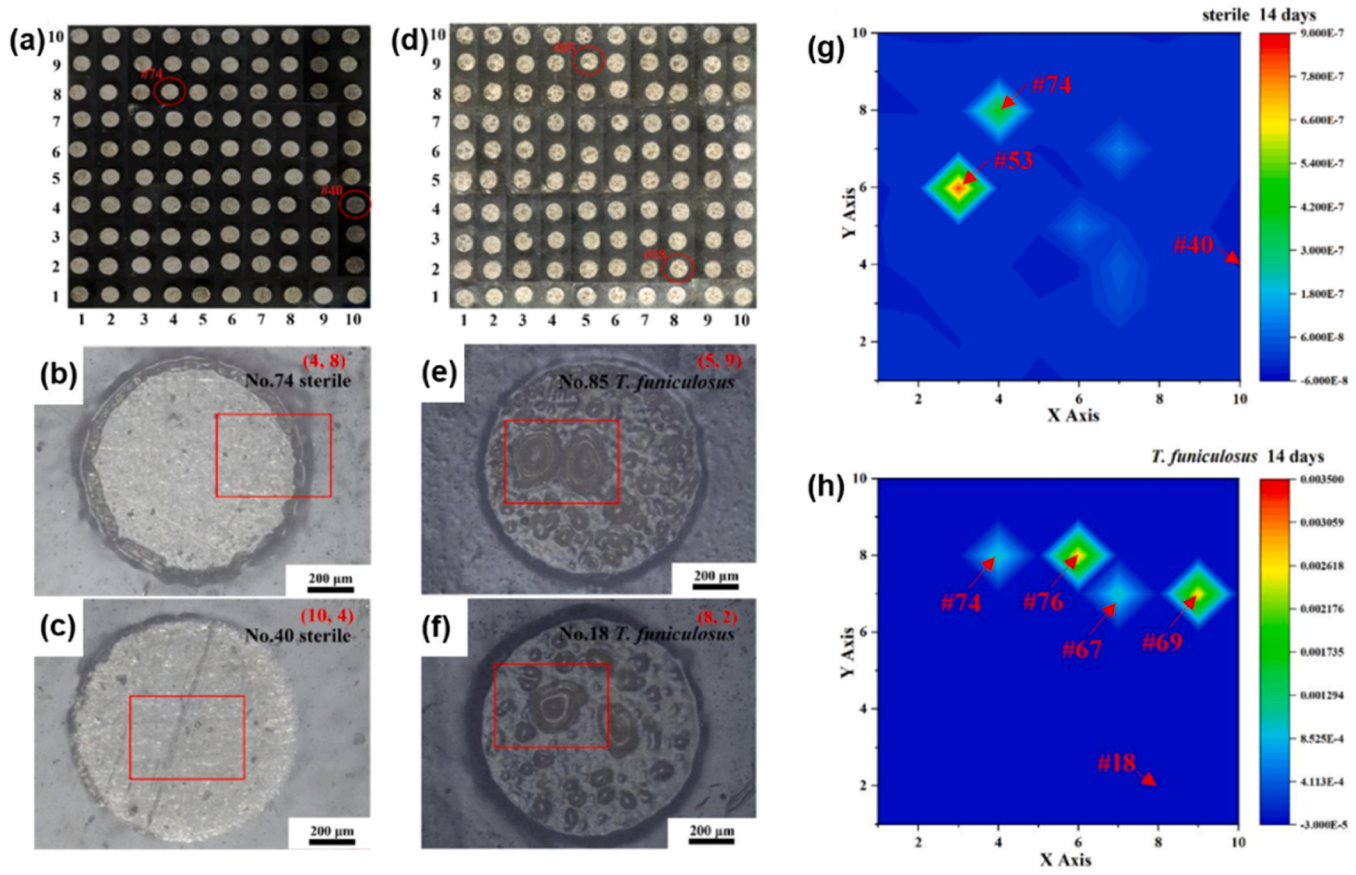

Fig. 15. Digital microscope images of the entire WBE surface after 14 days of immersion in the (**a**) sterile medium and (**d**) *T. funiculosus*-contained medium; Magnified images of localized WBE surface from the (**b**, **c**) sterile medium and (**e**, **f**) *T. funiculosus*-contained medium; Current density distribution of the entire WBE surface after the immersion in the (**g**) sterile medium and (**h**) *T. funiculosus*-contained medium for 14 days [114].

Table 1
Comparison of various localized electrochemical techniques [57,72,79].

Technique	Resolution	Resolution control	Detected signal	Advantages	Disadvantages
SECM	50 nm–20 μm	Tip size	Current/Potential	High spatial resolution; multiple operation modes	Current signal is influenced by the topography; simple redox species in electrolyte are required
SKP	> 50 μm	Tip size, Applied voltage	Contact potential difference	Accurate potential distribution detection	Real-time monitoring cannot be performed in solution; technical difficulties in the realization of high resolution
SKPFM	5 nm–1 μm	Applied voltage	Contact potential difference	High resolution; simultaneous acquisition of topography and potential distribution	Real-time monitoring cannot be performed in the solution
SVET	20 μm–200 μm	Vibration amplitude	Current	Avoidance of morphology interference	Lower resolution compared with SECM; repeated calibration with any change in solution conductivity; difficulty in vertical positioning
LEIS	10 μm–1 mm	Tip size	Impedance	Implementation in solution with complex composition	Lower resolution compared with SECM; difficulty in vertical positioning
WBE	> 0.5 mm	Diameter, quantity and arrangement of wires	Current, potential and impedance	High throughout detection of electrochemical information; continuous monitoring	Low resolution relative to the size of bacteria

adsorption and additional force such as buoyancy and drag force of the flow. Second, localized electrochemical techniques are unable to monitor the evolution of MIC over a long period of immersion time at present. The incubation of MIC requires a strictly enclosed environment to avoid environmental and microbial contamination, and needs specific temperature, humidity and oxygen concentration. In addition, detecting the distribution information of key corrosion factors, such as chloride ions and electron shuttles, within the biofilm poses a challenge for current localized electrochemical techniques. The microorganisms/material interface beneath the biofilm is the primary site for the occurrence of MIC. A variety of substances within the biofilm, including microbial cells and extracellular polymeric substances (EPS), can interfere with the positioning of probes and contaminate the tip of the probe.

To circumvent these problems, new attempts and designs of localized electrochemical aparatus are needed. (1) The combination of AFM and localized electrochemical methods, such as AFM-SECM, is expected to solve the problem of positioning difficulty. Its capability for dual measurement enables simultaneous mapping of electrode surface biofilm morphology and electrochemical signal distribution, helping to determine the source of the detected signal. The controllable detection height can realize precision three-dimensional electrochemical signal

collection (2) Soft probe and dual probes with ion-selective microelectrode hold promise for addressing issues of detection beneath biofilms by easy positioning operation and accurate detection of specific substances but present a certain difficulty in fabrication. In addition, using WBE as a substrate electrode and conducting scanning probe techniques, such as SECM or AFM, above substrate may be able to further comprehensively characterize the electrochemical signals from different aspects including the electrode, metal/biofilm interface, and biofilm side, providing a more holistic picture of MIC reactions beneath the biofilm. (3) According to existing reports, microorganisms will first adhere to the material surface and then gradually form a biofilm, which usually results in the fastest corrosion rate of the materials after 3–7 days of immersion. Continuous monitoring can provide insight into the whole process from microbial adhesion to biofilm formation and its impact on the degradation of materials. To this end, sensors based on the principle of localized electrochemistry are particularly needed to study the dynamic process of MIC during long-term laboratory microbial culture or even for field applications.

CRediT authorship contribution statement

Dawei Zhang: Writing – review & editing, Supervision. **Weiwei Chang:** Writing – original draft. **Hongchang Qian:** Writing – review & editing. **Ziyu Li:** Writing – review & editing. **Arjan Mol:** Writing – review & editing.

Declaration of Competing Interest

The authors declare that they have no known competing financial interests or personal relationships that could have appeared to influence the work reported in this paper.

Data Availability

No data was used for the research described in the article.

Acknowledgements

This work was supported by the National Natural Science Foundation of China (52161160308, 52071015, 52301074), National Key Research and Development Program of China (2023YFE0205300), and Guangdong Basic and Applied Basic Research Foundation (2021B1515130009).

References

[1] D.K. Xu, T.Y. Gu, D.R. Lovley, Microbially mediated metal corrosion, Nat. Rev. Microbiol. 21 (2023) 705–718.
[2] D.R. Lovley, Electrotrophy: other microbial species, iron, and electrodes as electron donors for microbial respirations, Bioresour. Technol. 345 (2022) 126553.
[3] M. Cámara, W. Green, C.E. MacPhee, P.D. Rakowska, R. Raval, M.C. Richardson, J. Slater-Jefferies, K. Steventon, J.S. Webb, Economic significance of biofilms: a multidisciplinary and cross-sectoral challenge, Npj Biofilms Micro 8 (2022).
[4] W. Beyerinck, Ueber Spirillum desulfuricans als ursache von sulfatreduction, 1895.
[5] H.C. Qian, S.Y. Li, W.L. Liu, P.F. Ju, D.W. Zhang, Microbiologically influenced corrosion of Q235 carbon steel by aerobic thermoacidophilic archaeon metallosphaera cuprina, Acta Met. Sin. -Engl. 35 (2022) 201–211.
[6] N.A. Chen, Q.Q. Liu, Y.L. Feng, S.W. Zou, Q. Yao, L. Lu, J.S. Wu, K. Xiao, Microbial corrosion behavior and mechanism of 5A06 aluminum alloy under low dose proton radiation, J. Mater. Res Technol. 27 (2023) 4533–4540.
[7] H.C. Qian, W.W. Chang, W.L. Liu, T.Y. Cui, Z. Li, D.W. Guo, C.T. Kwok, L.M. Tam, D.W. Zhang, Investigation of microbiologically influenced corrosion inhibition of 304 stainless steel by D-cysteine in the presence of Pseudomonas aeruginosa, Bioelectrochemistry 143 (2022).
[8] C. von Wolzogen Kühr, L. Van der Vlugt, The graphitization of cast iron as an electrobiochemical process in anaerobic soil, Water 18 (1934) 147–165.
[9] Y.A. Pu, Y.F. Cheng, W.W. Dou, Z.X. Xu, S. Hou, Y. Hou, S.G. Chen, Microbiologically influenced corrosion behavior of 70/30 Cu-Ni alloy exposed to carbon starvation environments with different aggressiveness: pitting mechanism induced by Desulfovibrio vulgaris, Corros. Sci. 222 (2023).
[10] W.W. Chang, Y.Y. Li, Z.Y. Li, Y.T. Lou, T.Y. Cui, H.C. Qian, A. Mol, D.W. Zhang, The effect of riboflavin on the microbiologically influenced corrosion of pure iron by Shewanella oneidensis MR-1, Bioelectrochemistry 147 (2022).
[11] W.W. Dou, Y.A. Pu, T.Y. Gu, S.G. Chen, Z.Y. Chen, Z.X. Xu, Biocorrosion of copper by nitrate reducing Pseudomonas aeruginosa with varied headspace volume, Int. Biodeter. Biodegr. 171 (2022).
[12] Y.T. Lou, C.D. Dai, W.W. Chang, H.C. Qian, L.Y. Huang, C.W. Du, D.W. Zhang, Microbiologically influenced corrosion of FeCoCrNiMo0.1 high-entropy alloys by marine Pseudomonas aeruginosa, Corros. Sci. 165 (2020).
[13] M.Y. Fu, X. Cheng, J.R. Li, S.Q. Chen, W.W. Dou, G.Z. Liu, Influence of soluble, loosely bound and tightly bound extracellular polymeric substances (EPS) produced by Desulfovibrio vulgaris on EH40 steel corrosion, Corros. Sci. 221 (2023).
[14] I. Lanneluc, M. Langumier, R. Sabot, M. Jeannin, P. Refait, S. Sablé, On the bacterial communities associated with the corrosion product layer during the early stages of marine corrosion of carbon steel, Int. Biodeter. Biodegr. 99 (2015) 55–65.
[15] G. O'Toole, H.B. Kaplan, R. Kolter, Biofilm formation as microbial development, Annu Rev. Microbiol. 54 (2000) 49–79.
[16] M. Moradi, Y. Gao, J. Narenkumar, Y.Q. Fan, T.Y. Gu, A.A. Carmona-Martinez, D. K. Xu, F.H. Wang, Filamentous marine Gram-positive Nocardiopsis dassonvillei biofilm as biocathode and its electron transfer mechanism, Sci. Total Environ. 908 (2024).
[17] H.W. Liu, X.K. Zhong, H.F. Liu, Y.F. Cheng, Microbiologically-enhanced galvanic corrosion of the steel beneath a deposit in simulated oilfield-produced water containing, Electrochem. Commun. 90 (2018) 1–5.
[18] B.J. Little, D.J. Blackwood, J. Hinks, F.M. Lauro, E. Marsili, A. Okamoto, S. A. Rice, S.A. Wade, H.C. Flemming, Microbially influenced corrosion—any progress? Corros. Sci. 170 (2020) 108641.
[19] Y.Q. Dong, B.T. Jiang, D.K. Xu, C.Y. Jiang, Q. Li, T.Y. Gu, Severe microbiologically influenced corrosion of S32654 super austenitic stainless steel by acid producing bacterium Acidithiobacillus caldus SM-1, Bioelectrochemistry 123 (2018) 34–44.
[20] J. Ress, G. Monrrabal, A. Díaz, J. Pérez-Pérez, J.M. Bastidas, D.M. Bastidas, Microbiologically influenced corrosion of welded AISI 304 stainless steel pipe in well water, Eng. Fail Anal. 116 (2020).
[21] E. Huttunen-Saarivirta, M. Honkanen, T. Lepistö, V.T. Kuokkala, L. Koivisto, C. G. Berg, Microbiologically influenced corrosion (MIC) in stainless steel heat exchanger, Appl. Surf. Sci. 258 (2012) 6512–6526.
[22] W.W. Chang, Z.Z. Tian, S.F. Jiang, M. Zhou, D.W. Guo, J.G. Gao, S.Y. He, C. T. Kwok, L.M. Tam, H.C. Qian, D.W. Zhang, Microbial corrosion of CoCrMnNi high entropy alloy by Pseudomonas aeruginosa through electron transfer between Mn and microbe, J. Mater. Res. Technol. 29 (2024) 386–399.
[23] K. Mori, H. Tsurumaru, S. Harayama, Iron corrosion activity of anaerobic hydrogen-consuming microorganisms isolated from oil facilities, J. Biosci. Bioeng. 110 (2010) 426–430.
[24] L. Shi, H.L. Dong, G. Reguera, H. Beyenal, A.H. Lu, J. Liu, H.Q. Yu, J. K. Fredrickson, Extracellular electron transfer mechanisms between microorganisms and minerals, Nat. Rev. Microbiol. 14 (2016) 651–662.
[25] Y.A. Pu, W.W. Dou, Y.F. Cheng, S.G. Chen, Z.X. Xu, Z.Y. Chen, Biogenic H2S and extracellular electron transfer resulted in two-coexisting mechanisms in 90/10 Cu-Ni alloy corrosion by a sulfate-reducing bacteria, Corros. Sci. 211 (2023).
[26] E.Z. Zhou, F. Li, D.W. Zhang, D.K. Xu, Z. Li, R. Jia, Y.T. Jin, H. Song, H.B. Li, Q. Wang, J.J. Wang, X.G. Li, T.Y. Gu, A.M. Homborg, J.M.C. Mol, J.A. Smith, F. H. Wang, D.R. Lovley, Direct microbial electron uptake as a mechanism for stainless steel corrosion in aerobic environments, Water Res. 219 (2022).
[27] B.J. Little, J. Hinks, D.J. Blackwood, Microbially influenced corrosion: Towards an interdisciplinary perspective on mechanisms, Int. Biodeter. Biodegr. (2020) 154.
[28] L. Daniels, N. Belay, B.S. Rajagopal, P.J. Weimer, Bacterial methanogenesis and growth from CO2 with elemental iron as the sole source of electrons, Science 237 (1987) 509–511.
[29] Y. Zhao, E.Z. Zhou, Y.Z. Liu, S.J. Liao, Z. Li, D.K. Xu, T. Zhang, T.Y. Gu, Comparison of different electrochemical techniques for continuous monitoring of the microbiologically influenced corrosion of 2205 duplex stainless steel by marine Pseudomonas aeruginosa biofilm, Corros. Sci. 126 (2017) 142–151.
[30] H.H. Wan, T.S. Zhang, J.L. Wang, Z. Rao, Y.Z. Zhang, G.F. Li, T.Y. Gu, H.F. Liu, Effect of alloying element content on anaerobic microbiologically influenced corrosion sensitivity of stainless steels in enriched artificial seawater, Bioelectrochemistry 150 (2023).
[31] J. Li, C.W. Du, Z.Y. Liu, X.G. Li, Electrochemical studies of microbiologically influenced corrosion of X80 steel by nitrate-reducing Bacillus licheniformis under anaerobic conditions, J. Mater. Sci. Technol. 118 (2022) 208–217.
[32] C. Nkoua, C. Josse, A. Proietti, R. Basseguy, C. Blanc, Corrosion behaviour of the microbially modified surface of 5083 aluminium alloy, Corros. Sci. 210 (2023).
[33] F. Mansfeld, The use of electrochemical techniques for the investigation and monitoring of microbiologically influenced corrosion and its inhibition - a review, Mater. Corros. 54 (2003) 489–502.
[34] F. Mansfeld, B. Little, A technical review of electrochemical techniques applied to microbiologically influenced corrosion, Corros. Sci. 32 (1991) 247–272.
[35] E. Juzeliunas, R. Ramanauskas, A. Lugauskas, K. Leinartas, M. Samuleviciene, A. Sudavicius, R. Juskenas, Microbially influenced corrosion of zinc and aluminium: two-year subjection to influence of Aspergillus niger, Corros. Sci. 49 (2007) 4098–4112.
[36] H.C. Qian, W.W. Chang, T.Y. Cui, Z. Li, D.W. Guo, C.T. Kwok, L.M. Tam, D. W. Zhang, Multi-mode scanning electrochemical microscopic study of

microbiologically influenced corrosion mechanism of 304 stainless steel by thermoacidophilic archaea, Corros. Sci. 191 (2021).
[37] A.J. Bard, F.R.F. Fan, J. Kwak, O. Lev, Scanning electrochemical microscopy. Introduction and principles, Anal. Chem. 61 (1989) 132–138.
[38] R.C. Engstrom, C.M. Pharr, Scanning electrochemical microscopy, Anal. Chem. 61 (1989) 1099A–1104A.
[39] G. Caniglia, C. Kranz, Scanning electrochemical microscopy and its potential for studying biofilms and antimicrobial coatings, Anal. Bioanal. Chem. 412 (2020) 6133–6148.
[40] J.Q. Feng, Y.B. Wang, X.L. Lin, M.H. Bian, Y.Z. Wei, SECM in situ investigation of corrosion and self-healing behavior of trivalent chromium conversion coating on the zinc, Surf. Coat. Tech. 459 (2023).
[41] W. Nogala, K. Szot, M. Burchardt, F. Roelfs, J. Rogalski, M. Opallo, G. Wittstock, Feedback mode SECM study of laccase and bilirubin oxidase immobilised in a sol-gel processed silicate film, Analyst 135 (2010) 2051–2058.
[42] C.G. Zoski, Ultramicroelectrodes: design, fabrication, and characterization, Electroanal 14 (2002) 1041–1051.
[43] L.Y. Huang, Z.Y. Li, Y.T. Lou, F.H. Cao, D.W. Zhang, X.G. Li, Recent advances in scanning electrochemical microscopy for biological applications, Materials 11 (2018).
[44] M.V. Mirkin, W. Nogala, J. Velmurugan, Y.X. Wang, Scanning electrochemical microscopy in the 21st century. Update 1: five years after, Phys. Chem. Chem. Phys. 13 (2011) 21196–21212.
[45] R. Cornut, C. Lefrou, A unified new analytical approximation for negative feedback currents with a microdisk SECM tip, J. Electro Chem. 608 (2007) 59–66.
[46] I. Morkvenaite-Vilkonciene, A. Ramanaviciene, A. Ramanavicius, Redox competition and generation-collection modes based scanning electrochemical microscopy for the evaluation of immobilised glucose oxidase-catalysed reactions, Rsc Adv. 4 (2014) 50064–50069.
[47] J.J. Santana, J. González-Guzmán, L. Fernández-Mérida, S. González, R.M. Souto, Visualization of local degradation processes in coated metals by means of scanning electrochemical microscopy in the redox competition mode, Electro Acta 55 (2010) 4488–4494.
[48] A. Asserghine, M. Medvidovic-Kosanovic, L. Nagy, R.M. Souto, G. Nagy, A study of the electrochemical reactivity of titanium under cathodic polarization by means of combined feedback and redox competition modes of scanning electrochemical microscopy, Sens. Actuat. B-Chem. 320 (2020).
[49] Z.Y. Li, W.W. Chang, T.Y. Cui, D.K. Xu, D.W. Zhang, Y.T. Lou, H.C. Qian, H. Song, A. Mol, F.H. Cao, T.Y. Gu, X.G. Li, Adaptive bidirectional extracellular electron transfer during accelerated microbiologically influenced corrosion of stainless steel, Commun. Mater. 2 (2021).
[50] L.Y. Huang, W.W. Chang, D.W. Zhang, Y. Huang, Z.Y. Li, Y.T. Lou, H.C. Qian, C. Y. Jiang, X.G. Li, A. Mol, Acceleration of corrosion of 304 stainless steel by outward extracellular electron transfer of Pseudomonas aeruginosa biofilm, Corros. Sci. 199 (2022).
[51] Z.J. Zhu, Q.H. Zhang, P. Liu, J.Q. Zhang, F.H. Cao, Quasi-simultaneous electrochemical/chemical imaging of local Fe and pH distributions on 316 L stainless steel surface, J. Electro Chem. 871 (2020).
[52] D. Harris, J.G. Ummadi, A.R. Thurber, Y. Allau, C. Verba, F. Colwell, M.E. Torres, D. Koley, Real-time monitoring of calcification process by Sporosarcina pasteurii biofilm, Analyst 141 (2016) 2887–2895.
[53] Z.J. Zhu, Z.N. Ye, Q.H. Zhang, J.Q. Zhang, F.H. Cao, Novel dual Pt-Pt/IrOx ultramicroelectrode for pH imaging using SECM in both potentiometric and amperometric modes, Electrochem Commun. 88 (2018) 47–51.
[54] P. Actis, S. Tokar, J. Clausmeyer, B. Babakinejad, S. Mikhaleva, R. Cornut, Y. Takahashi, A.L. Córdoba, P. Novak, A.I. Shevchuck, J.A. Dougan, S. G. Kazarian, P.V. Gorelkin, A.S. Erofeev, I.V. Yaminsky, P.R. Unwin, W. Schuhmann, D. Klenerman, D.A. Rusakov, E.V. Sviderskaya, Y.E. Korchev, Electrochemical nanoprobes for single-cell analysis, Acs Nano 8 (2014) 875–884.
[55] E.E.D.M. El-Giar, D.O. Wipf, Microparticle-based iridium oxide ultramicroelectrodes for pH sensing and imaging, J. Electro Chem. 609 (2007) 147–154.
[56] S. Darvishi, H. Pick, E. Oveisi, H.H. Girault, A. Lesch, Soft-probe-scanning electrochemical microscopy reveals electrochemical surface reactivity of E. coli biofilms, Sens. Actuat. B-Chem. 334 (2021).
[57] D.Q. Liu, B.X. Zhang, G.Q. Zhao, J. Chen, H.G. Pan, W.P. Sun, Advanced in-situ electrochemical scanning probe microscopies in electrocatalysis, Chin. J. Catal. 47 (2023) 93–120.
[58] J. Park, J.H. Lim, J.H. Kang, J. Lim, H.W. Jang, H. Shin, S.H. Park, A review of understanding electrocatalytic reactions in energy conversion and energy storage systems via scanning electrochemical microscopy, J. Energy Chem. 91 (2024) 155–177.
[59] L. Kelvin, V. Contact electricity of metals, Lond., Edinb., Dublin Philos. Mag. J. Sci. 46 (1898) 82–120.
[60] C. Örnek, C. Leygraf, J. Pan, On the Volta potential measured by SKPFM – fundamental and practical aspects with relevance to corrosion science, Corros. Eng. Sci. Technol. 54 (2019) 185–198.
[61] M. Stratmann, The investigation of the corrosion properties of metals, covered with adsorbed electrolyte layers—a new experimental technique, Corros. Sci. 27 (1987) 869–872.
[62] M.S.B. Reddy, D. Ponnamma, K.K. Sadasivuni, S. Aich, S. Kailasa, H. Parangusan, M. Ibrahim, S. Eldeib, O. Shehata, M. Ismail, R. Zarandah, Sensors in advancing the capabilities of corrosion detection: a review, Sens. Actuat. A-Phys. 332 (2021).
[63] M.C.L. de Oliveira, R.M.P. da Silva, R.M. Souto, R.A. Antunes, Investigating local corrosion processes of magnesium alloys with scanning probe electrochemical techniques: a review, J. Magnes. Alloy 10 (2022) 2997–3030.
[64] S. Yee, R.A. Oriani, M. Stratmann, Application of a kelvin microprobe to the corrosion of metals in humid atmospheres, J. Electrochem Soc. 138 (1991) 55.
[65] F. Mandavi, M. Forsyth, M.Y.J. Tan, Techniques for testing and monitoring the cathodic disbondment of organic coatings: An overview of major obstacles and innovations, Prog. Org. Coat. 105 (2017) 163–175.
[66] M. Nonnenmacher, M. o'Boyle, H.K. Wickramasinghe, Kelvin probe force microscopy, Appl. Phys. Lett. 58 (1991) 2921–2923.
[67] Q.C. Zhao, Z.M. Pan, X.F. Wang, H. Luo, Y. Liu, X.G. Li, Corrosion and passive behavior of AlxCrFeNi3-x (x=0.6, 0.8, 1.0) eutectic high entropy alloys in chloride environment, Corros. Sci. 208 (2022).
[68] W.W. Chang, X.Y. Wang, H.C. Qian, X.D. Chen, Y.T. Lou, M. Zhou, D.W. Guo, C. T. Kwok, L.M. Tam, D.W. Zhang, Effect of Sn addition on microstructure, hardness and corrosion behavior of CoCrFeNiSnx high entropy alloys in chloride environment, Corros. Sci. 227 (2024).
[69] D. Guo, J. Chen, X. Chen, Q. Shi, V.A.M. Cristino, C.T. Kwok, L.M. Tam, H. Qian, D. Zhang, X. Li, Pitting corrosion behavior of friction-surfaced 17-4PH stainless steel coatings with and without subsequent heat treatment, Corros. Sci. 193 (2021).
[70] P. Schmutz, G.S. Frankel, Corrosion study of AA2024-T3 by scanning Kelvin probe force microscopy and in situ atomic force microscopy scratching, J. Electrochem Soc. 145 (1998) 2295–2306.
[71] V. Guillaumin, P. Schmutz, G.S. Frankel, Characterization of corrosion interfaces by the scanning Kelvin probe force microscopy technique, J. Electrochem Soc. 148 (2001) B163–B173.
[72] M. Rohwerder, F. Turcu, High-resolution Kelvin probe microscopy in corrosion science: scanning Kelvin probe force microscopy (SKPFM) versus classical scanning Kelvin probe (SKP), Electro Acta 53 (2007) 290–299.
[73] H.S. Isaacs, The use of the scanning vibrating electrode technique for detecting defects in ion vapor-deposited aluminum on steel, Corros. US 43 (1987) 594–596.
[74] J. Izquierdo, L. Martín-Ruíz, B.M. Fernández-Pérez, L. Fernández-Mérida, J. J. Santana, R.M. Souto, Imaging local surface reactivity on stainless steels 304 and 316 in acid chloride solution using scanning electrochemical microscopy and the scanning vibrating electrode technique, Electro Acta 134 (2014) 167–175.
[75] A.I. Ikeuba, Bimetallic corrosion evaluation of the π-Al8Mg3FeSi6 phase/Al couple in acidic, neutral and alkaline aqueous solutions using the scanning vibrating electrode technique, Electro Acta 449 (2023) 142240.
[76] D.V. Andreeva, D. Fix, H. Möhwald, D.G. Shchukin, Self-healing anticorrosion coatings based on pH-sensitive polyelectrolyte/inhibitor sandwichlike nanostructures, Adv. Mater. 20 (2008) 2789.
[77] A.C. Bastos, M.C. Quevedo, O.V. Karavai, M.G.S. Ferreira, On the application of the scanning vibrating electrode technique (SVET) to corrosion research, J. Electrochem Soc. 164 (2017) C973–C990.
[78] W.Z. Wei, K.M. Wu, X. Zhang, J. Liu, P. Qiu, L. Cheng, In-situ characterization of initial marine corrosion induced by rare-earth elements modified inclusions in Zr-Ti deoxidized low-alloy steels, J. Mater. Res. Technol. 9 (2020) 1412–1424.
[79] L. Grandy, J. Mauzeroll, Localising the electrochemistry of corrosion fatigue, Curr. Opin. Colloid 61 (2022).
[80] A.C. Bastos, M.C. Quevedo, M.G.S. Ferreira, The influence of vibration and probe movement on SVET measurements, Corros. Sci. 92 (2015) 309–314.
[81] R. Lillard, P. Moran, H. Isaacs, A novel method for generating quantitative local electrochemical impedance spectroscopy, J. Electrochem. Soc. 139 (1992) 1007.
[82] V.M. Huang, S.L. Wu, M.E. Orazem, N. Pébère, B. Tribollet, V. Vivier, Local electrochemical impedance spectroscopy: a review and some recent developments, Electro Acta 56 (2011) 8048–8057.
[83] F. Zou, D. Thierry, H.S. Isaacs, A high-resolution probe for localized electrochemical impedance spectroscopy measurements, J. Electrochem. Soc. 144 (1997) 1957–1965.
[84] O. Gharbi, K. Ngo, M. Turmine, V. Vivier, Local electrochemical impedance spectroscopy: a window into heterogeneous interfaces, Curr. Opin. Electro 20 (2020) 1–7.
[85] V.M.-W. Huang, V. Vivier, M.E. Orazem, N. Pébère, B. Tribollet, The apparent constant-phase-element behavior of an ideally polarized blocking electrode: a global and local impedance analysis, J. Electrochem. Soc. 154 (2007) C81.
[86] C.G. Zoski, Review—advances in scanning electrochemical microscopy (SECM), J. Electrochem. Soc. 163 (2016) H3088.
[87] G.Y. Feng, Z.Q. Jin, D.J. Zhu, C.S. Xiong, Z. Li, X.X. Wang, Corrosion propagation of steel reinforcement in pre-cracked mortar attacked by seawater using wire beam electrode, Corros. Sci. 208 (2022).
[88] D. Battocchi, J. He, G.P. Bierwagen, D.E. Tallman, Emulation and study of the corrosion behavior of Al alloy 2024-T3 using a wire beam electrode (WBE) in conjunction with scanning vibrating electrode technique (SVET), Corros. Sci. 47 (2005) 1165–1176.
[89] N.N. Aung, Y.J. Tan, A new method of studying buried steel corrosion and its inhibition using the wire beam electrode, Corros. Sci. 46 (2004) 3057–3067.
[90] W. Shi, T.Z. Wang, Z.H. Dong, X.P. Guo, Application of wire beam electrode technique to investigate the migrating behavior of corrosion inhibitors in mortar, Constr. Build. Mater. 134 (2017) 167–175.
[91] Y.-J. Tan, The effects of inhomogeneity in organic coatings on electrochemical measurements using a wire beam electrode: Part I, Prog. Org. Coat. 19 (1991) 89–94.
[92] Y.-J. Tan, S. Bailey, B. Kinsella, Mapping non-uniform corrosion using the wire beam electrode method. I. Multi-phase carbon dioxide corrosion, Corros. Sci. 43 (2001) 1905–1918.

[93] Y.J. Tan, N.N. Aung, T. Liu, Evaluating localised corrosion intensity using the wire beam electrode, Corros. Sci. 63 (2012) 379–386.
[94] J.L. Connell, J. Kim, J.B. Shear, A.J. Bard, M. Whiteley, Real-time monitoring of quorum sensing in 3D-printed bacterial aggregates using scanning electrochemical microscopy, P Natl. Acad. Sci. USA 111 (2014) 18255–18260.
[95] R. Moreira, M.K. Schütz, M. Libert, B. Tribollet, V. Vivier, Influence of hydrogen-oxidizing bacteria on the corrosion of low carbon steel: Local electrochemical investigations, Bioelectrochemistry 97 (2014) 69–75.
[96] Y.T. Lou, W.W. Chang, T.Y. Cui, H.C. Qian, L.Y. Huang, L.W. Ma, X.P. Hao, D. W. Zhang, Microbiologically influenced corrosion inhibition of carbon steel via biomineralization induced by Shewanella putrefaciens, Npj Mat. Degrad. 5 (2021).
[97] B. Liu, Z.Y. Li, X.J. Yang, C.W. Du, X.G. Li, Microbiologically influenced corrosion of X80 pipeline steel by nitrate reducing bacteria in artificial Beijing soil, Bioelectrochemistry 135 (2020).
[98] B. Liu, M.H. Sun, F.Y. Lu, C.W. Du, X.G. Li, Study of biofilm-influenced corrosion on X80 pipeline steel by a nitrate-reducing bacterium, Bacillus cereus, in artificial Beijing soil, Colloid Surf. B 197 (2021).
[99] T.Y. Cui, H.C. Qian, W.W. Chang, H.B. Zheng, D.W. Guo, C.T. Kwok, L.M. Tam, D. W. Zhang, Towards understanding Shewanella algae-induced degradation of passive film of stainless steel based on electrochemical, XPS and multi-mode AFM analyses, Corros. Sci. 218 (2023).
[100] T.Y. Cui, H.C. Qian, Y.T. Lou, X.D. Chen, T. Sun, D.W. Zhang, X.G. Li, Single-cell level investigation of microbiologically induced degradation of passive film of stainless steel via FIB-SEM/TEM and multi-mode AFM, Corros. Sci. 206 (2022).
[101] Y.T. Lou, W.W. Chang, T.Y. Cui, H.C. Qian, X.P. Hao, D.W. Zhang, Microbiologically influenced corrosion inhibition induced by S. putriefaciens mineralization under extracellular polymeric substance regulation via FlrA and FlhG genes, Corros. Sci. 221 (2023).
[102] M.J. Franklin, D.C. White, H.S. Isaacs, Pitting corrosion by bacteria on carbon steel, determined by the scanning vibrating electrode technique, Corros. Sci. 32 (1991) 945–952.
[103] T. Liu, Y.F. Cheng, M. Sharma, G. Voordouw, Effect of fluid flow on biofilm formation and microbiologically influenced corrosion of pipelines in oilfield produced water, J. Pet. Sci. Eng. 156 (2017) 451–459.
[104] Z.W. Guo, T. Liu, Y.F. Cheng, N. Guo, Y.S. Yin, Adhesion of Bacillus subtilis and Pseudoalteromonas lipolytica to steel in a seawater environment and their effects on corrosion, Colloid Surf. B 157 (2017) 157–165.
[105] I. Ziadi, M.M. Alves, M. Taryba, L. El-Bassi, H. Hassairi, L. Bousselmi, M. F. Montemor, H. Akrout, Microbiologically influenced corrosion mechanism of 304L stainless steel in treated urban wastewater and protective effect of silane-TiO2 coating, Bioelectrochemistry 132 (2020).
[106] Y.Y. Shen, Y.H. Dong, Y. Yang, Q.H. Li, H.L. Zhu, W.T. Zhang, L.H. Dong, Y.S. Yin, Study of pitting corrosion inhibition effect on aluminum alloy in seawater by biomineralized film, Bioelectrochemistry 132 (2020).
[107] Z.H. Dong, W. Shi, H.M. Ruan, G.A. Zhang, Heterogeneous corrosion of mild steel under SRB-biofilm characterised by electrochemical mapping technique, Corros. Sci. 53 (2011) 2978–2987.
[108] S.Q. Chen, P. Wang, D. Zhang, Corrosion behavior of copper under biofilm of sulfate-reducing bacteria, Corros. Sci. 87 (2014) 407–415.
[109] C. Wu, Z. Wang, Z. Zhang, B. Zhang, G. Ma, Q. Yao, Z. Gan, J. Wu, X. Li, Influence of crevice width on sulfate-reducing bacteria (SRB)-induced corrosion of stainless steel 316L, Corros. Commun. 4 (2021) 33–44.
[110] S.Q. Chen, D. Zhang, Effects of metabolic activity of sulphate-reducing bacteria on heterogeneous corrosion behaviors of copper in seawater, Mater. Corros. 69 (2018) 985–997.
[111] L.X. Wei, Y. Ge, Q.H. Gao, C. Wang, X. Yu, L. Zhang, Effect of salt-resistant polymer flooding system SRB on corrosion behavior of 20# carbon steel under deposition, J. Electro Chem. (2022) 921.
[112] H.X. Liu, Z.Y. Jin, Z. Wang, H.F. Liu, G.Z. Meng, H.W. Liu, Corrosion inhibition of deposit-covered X80 pipeline steel in seawater containing Pseudomonas stutzeri, Bioelectrochemistry 149 (2023).
[113] B. Tuck, E. Watkin, A. Somers, M. Forsyth, L.L. Machuca, Conditioning of metal surfaces enhances Shewanella chilikensis adhesion, Biofouling 38 (2022) 207–222.
[114] X.P. Hao, K.X. Yang, Y.D. Yuan, D.W. Zhang, L. Lu, Investigating different local polyurethane coatings degradation effects and corrosion behaivors by talaromyces funiculosus via wire beam electrodes, Materials 16 (2023).